

anisotropy of TeV cosmic rays and the outer heliospheric boundaries

Paolo Desiati^{1,2} [<desiati@wipac.wisc.edu>](mailto:desiati@wipac.wisc.edu)

Alexander Lazarian²

¹ WIPAC - Wisconsin IceCube Particle Astrophysics Center

² Department of Astronomy

University of Wisconsin - Madison



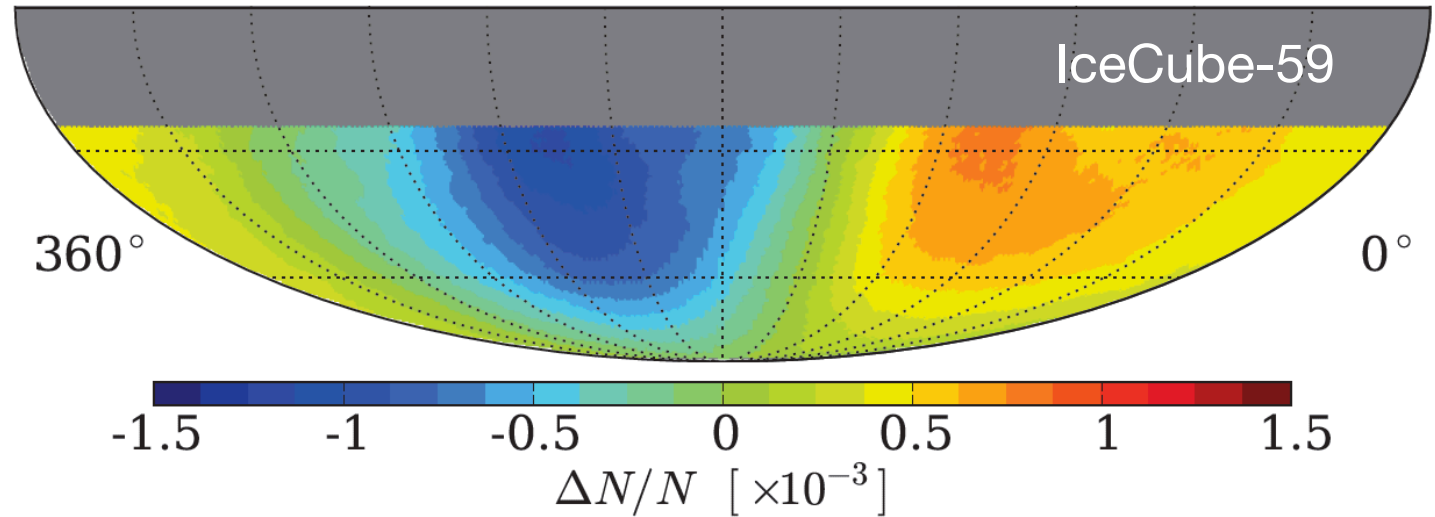
Playa Del Carmen, Mexico
February 7
2013
1

cosmic ray anisotropy large scale

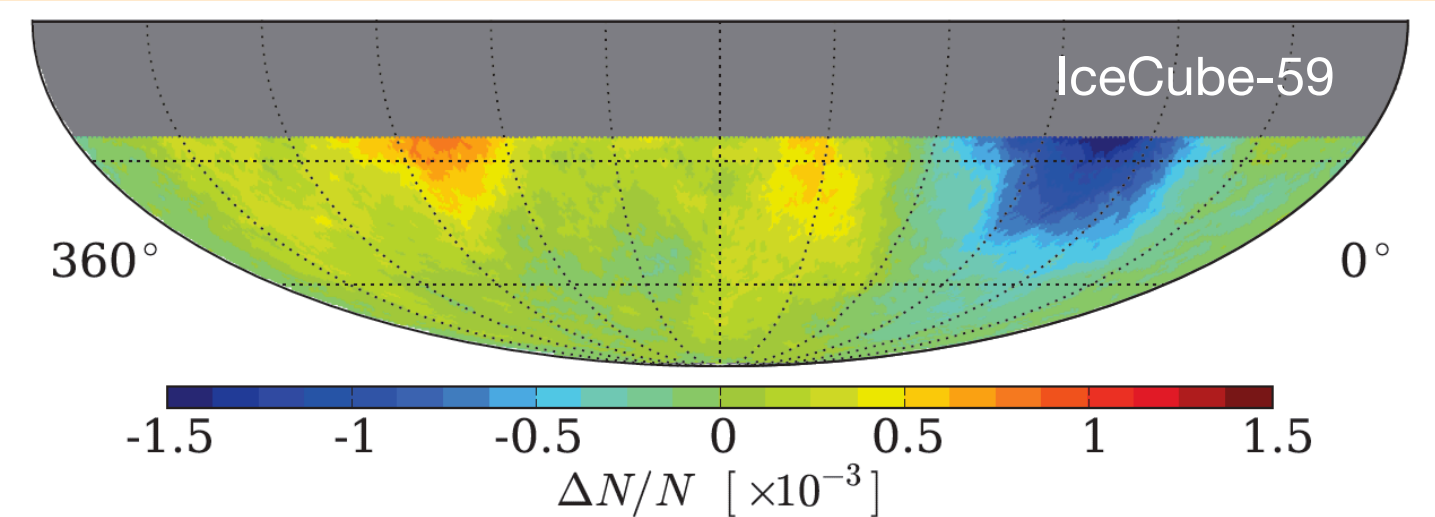
Abbasi et al., ApJ, **718**, L194, 2010
 Abbasi et al., ApJ, **746**, 33, 2012
 Aartsen et al., arXiv:1210.5278
 accepted to ApJ

relative intensity

equatorial coordinates

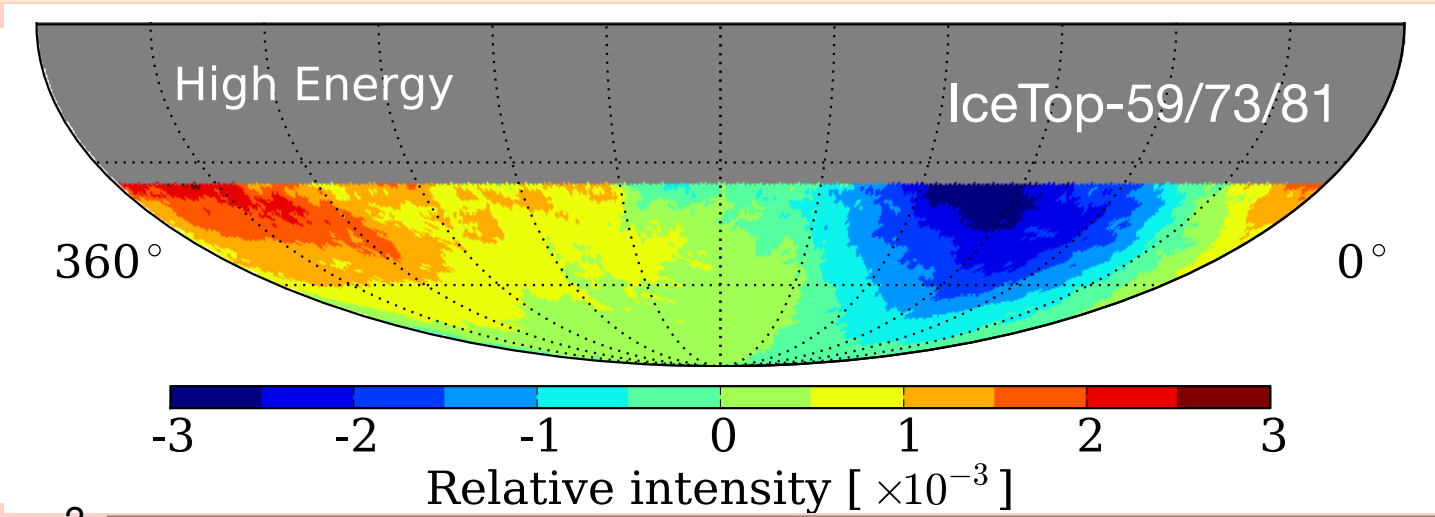


20 TeV



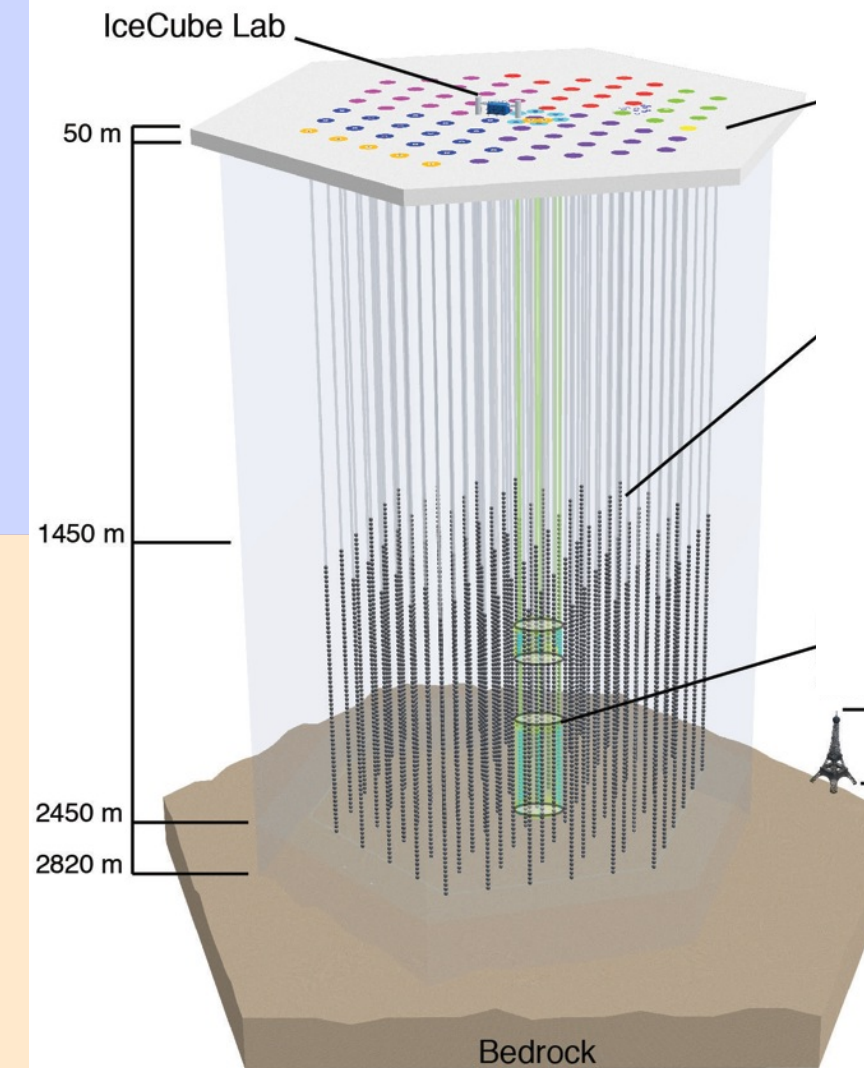
400 TeV

deficit
6.3 σ



2 PeV

deficit
7 σ



$$\frac{\Delta I}{\langle I \rangle} \equiv \frac{N_i - \langle N \rangle}{\langle N \rangle}$$

NOT A DIPOLE
ANISOTROPY

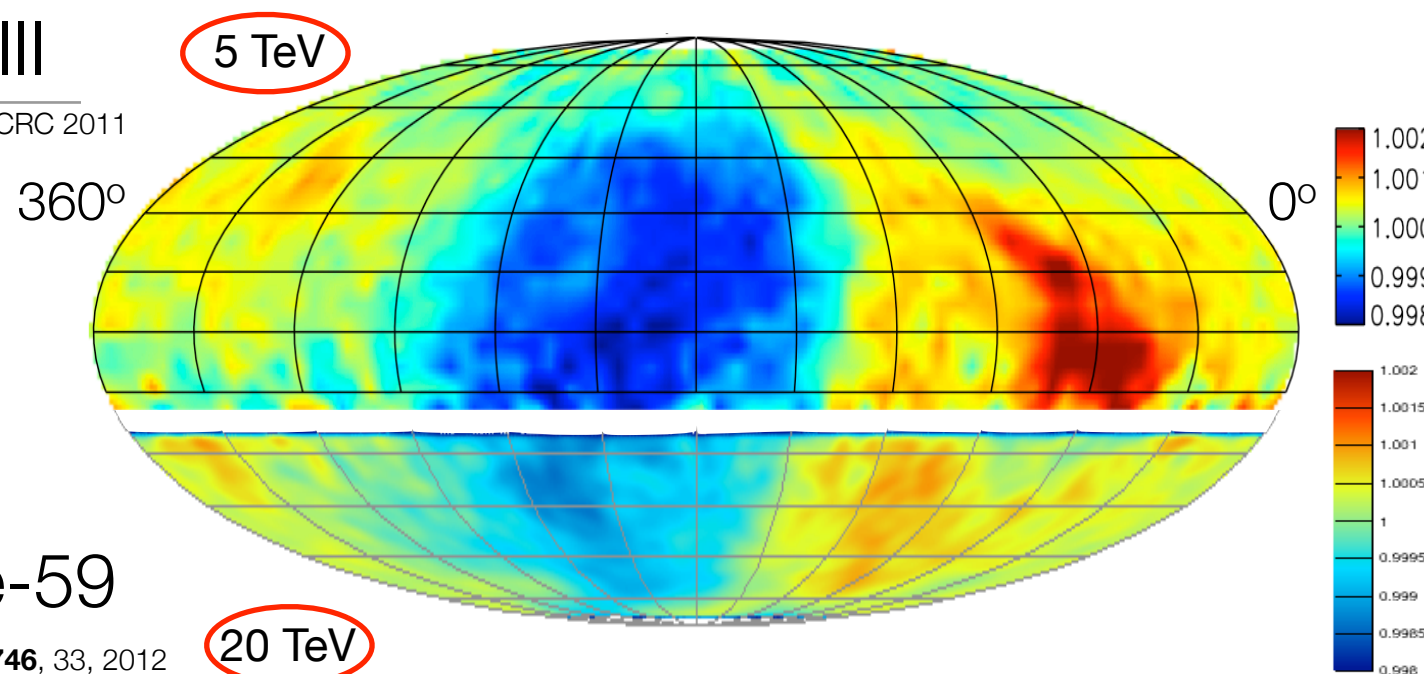
Paolo Desiati

cosmic ray anisotropy large scale → small scale

II

Tibet-III

Amenomori et al., ICRC 2011



equatorial coordinates

relative intensity

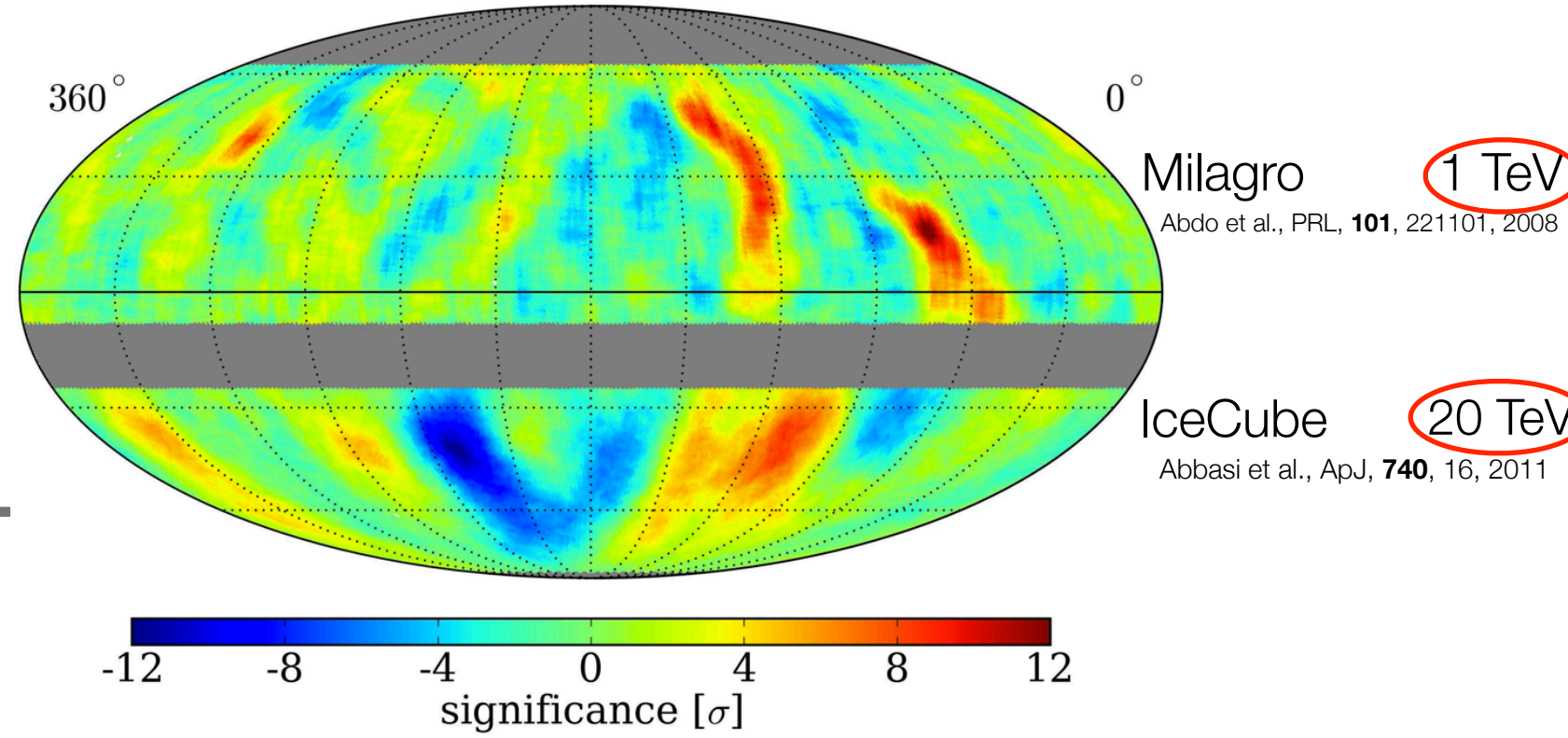
IceCube-59

Abbasi et al., ApJ, 746, 33, 2012

20 TeV

Milagro + IceCube TeV Cosmic Ray Data (10° Smoothing)

$2 \text{ hr} = 30^\circ$

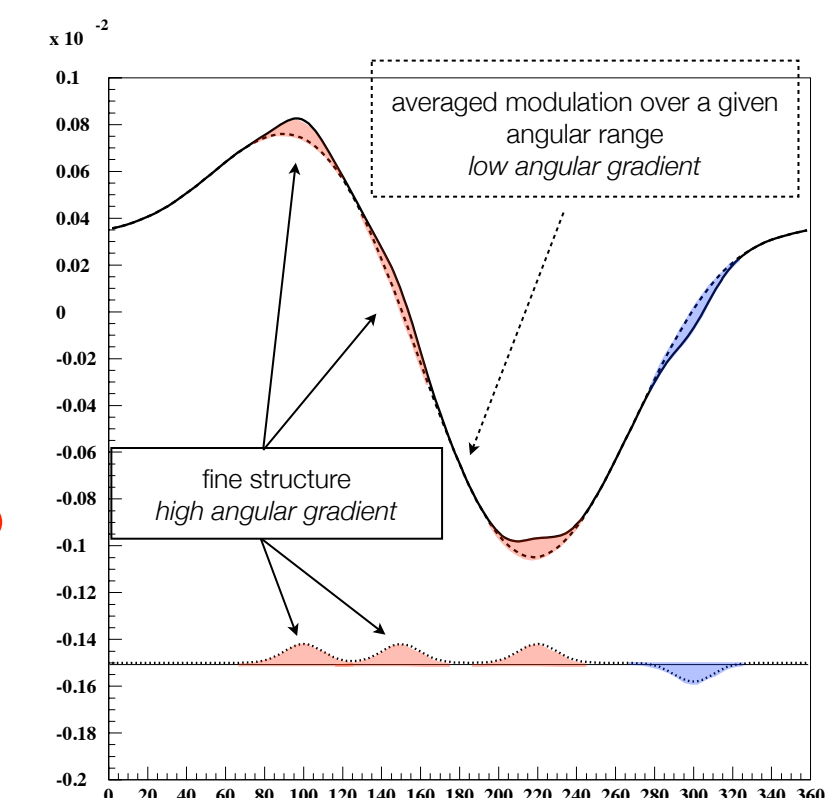


Milagro

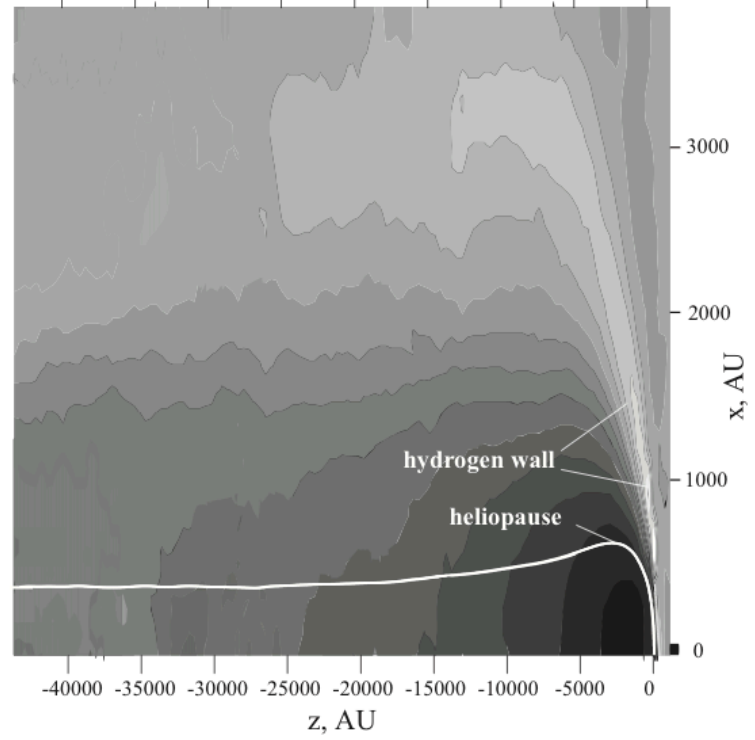
Abdo et al., PRL, 101, 221101, 2008

IceCube

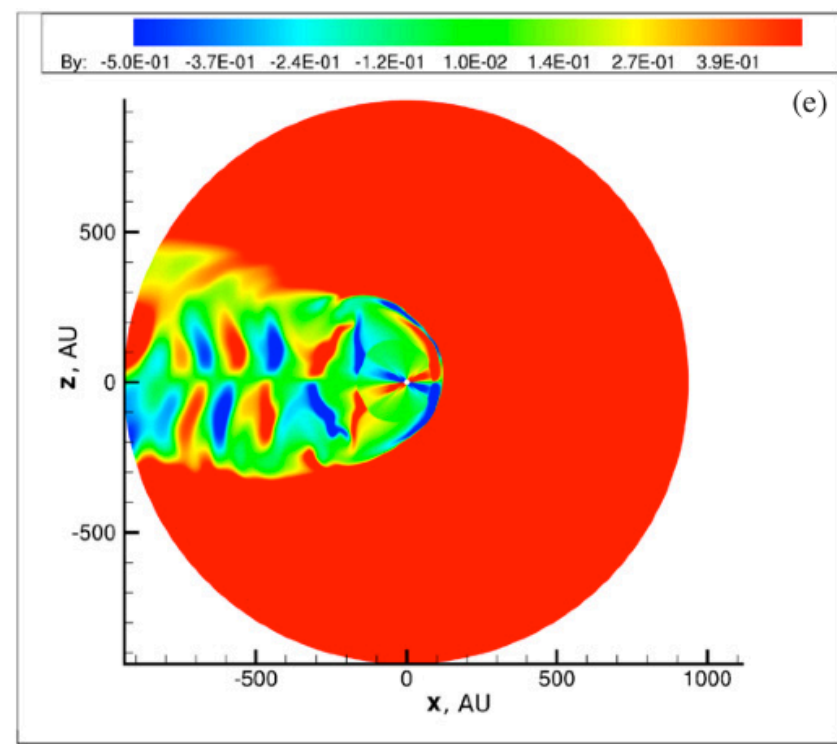
Abbasi et al., ApJ, 740, 16, 2011



cosmic ray anisotropy heliospheric influence

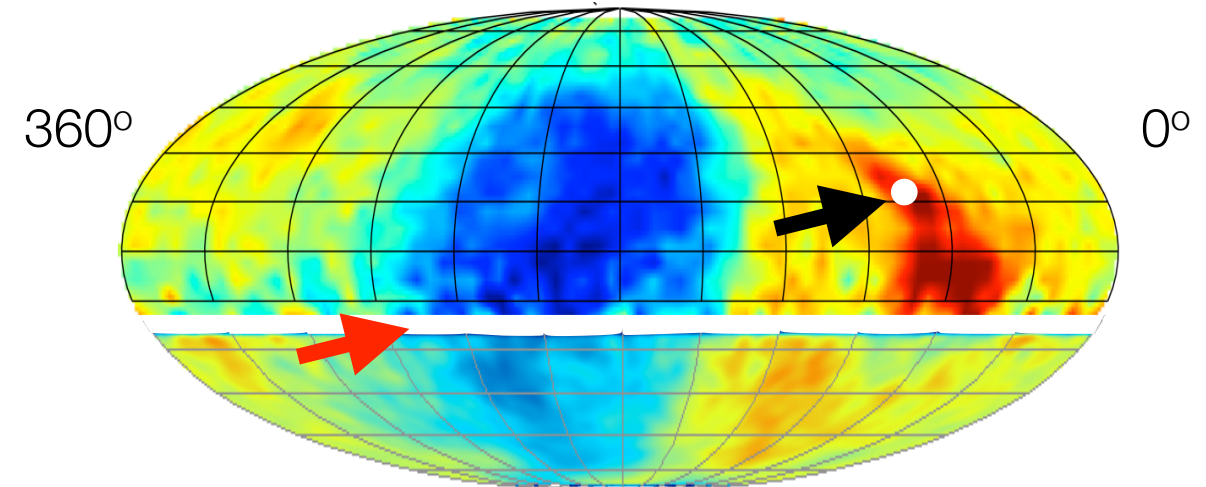
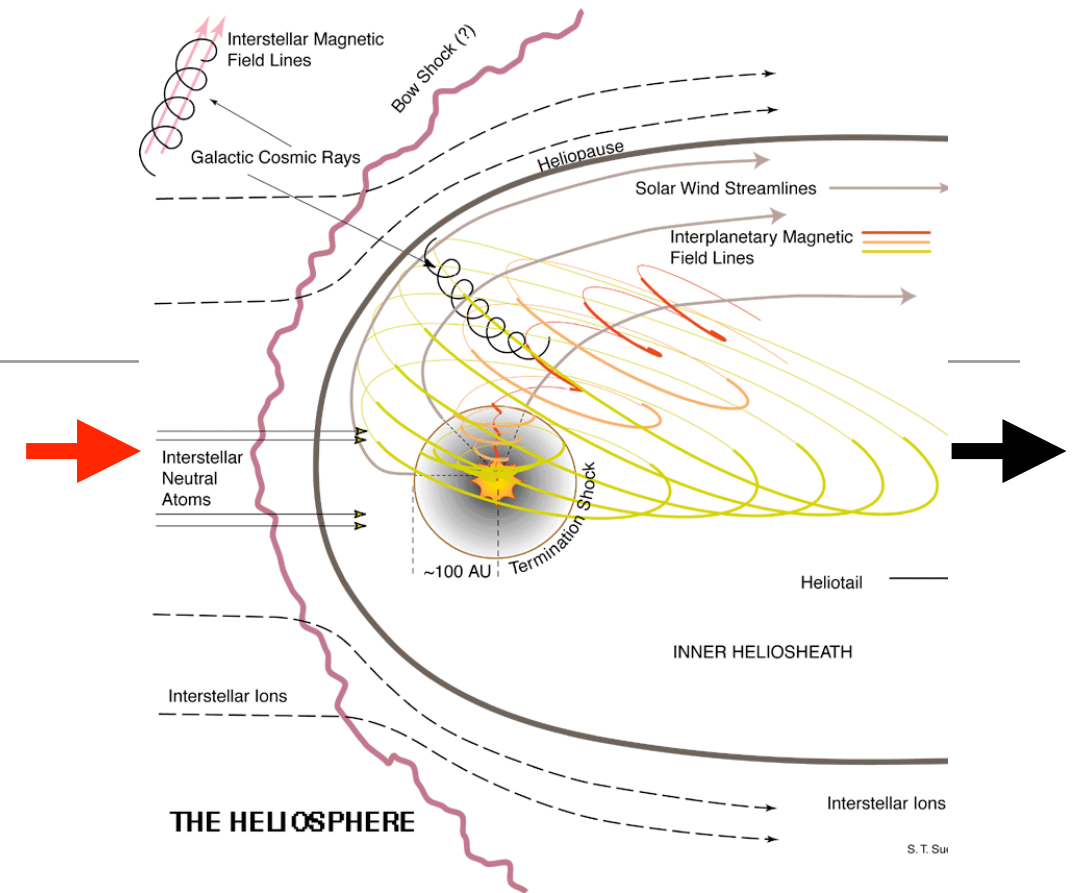


Izmodenov+ 2003



Pogorelov+ 2009

4



heliospheric size of $O(100\text{-}10,000) \text{ AU}$ influences
cosmic rays up to $O(10\text{-}100) \text{ TeV}$

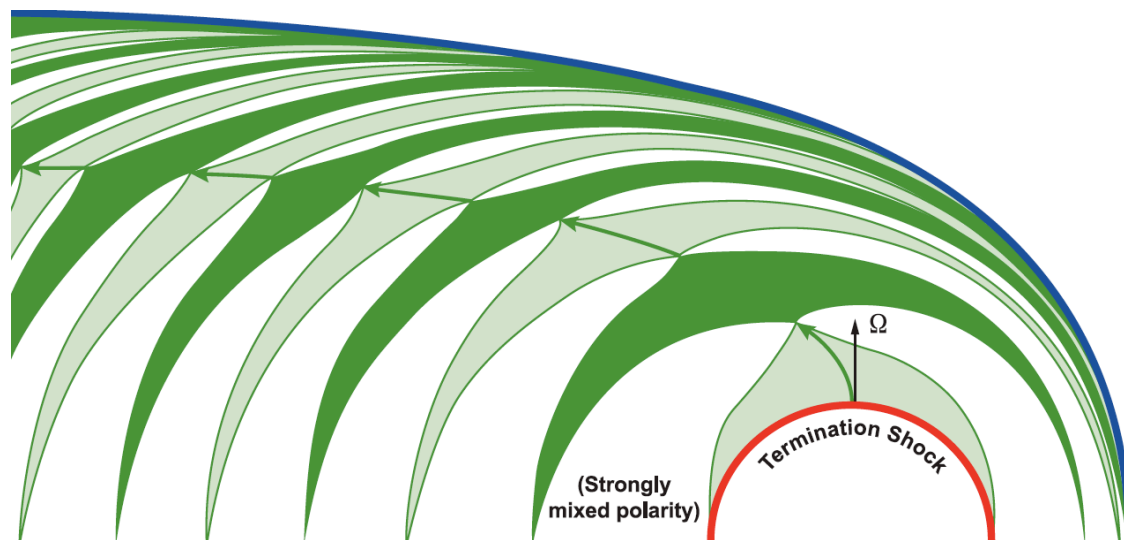
Paolo Desiati

heliospheric perturbations solar cycles

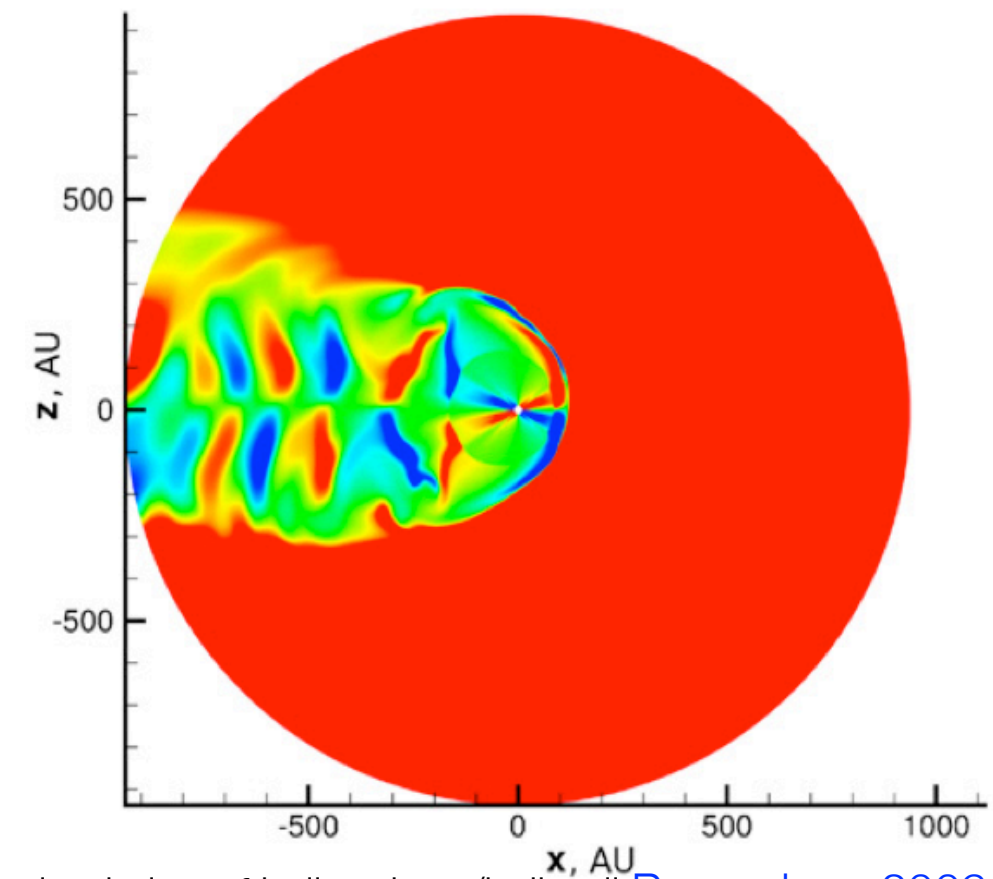
- solar wind modulated over a solar cycle, affecting heliospheric dynamics

Zank & Müller 2003
Pogorelov+ 2009
Washimi+ 2011, 2012

- complex heliotail structure shaped by solar cycles

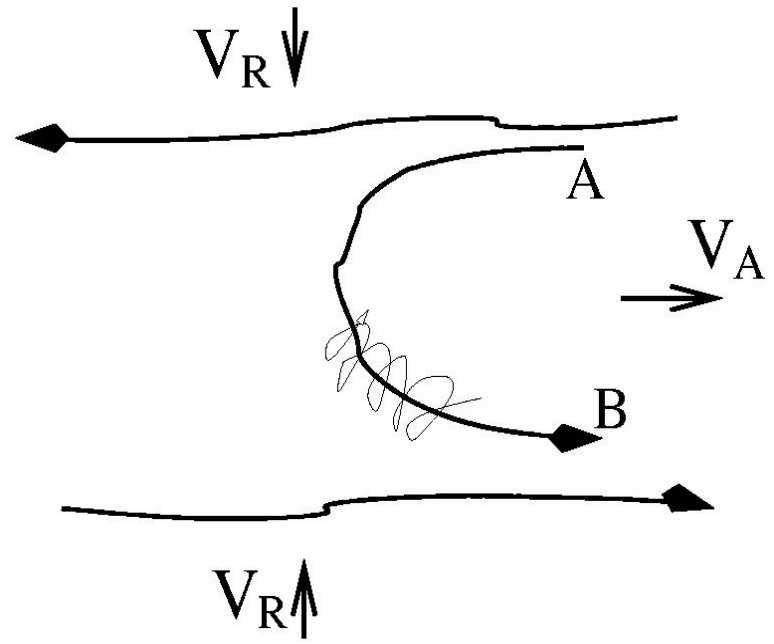


Nerney & Suess 1995



3D simulation of heliosphere/heliotail Pogorelov+ 2009

cosmic ray anisotropy & acceleration stochastic magnetic reconnection



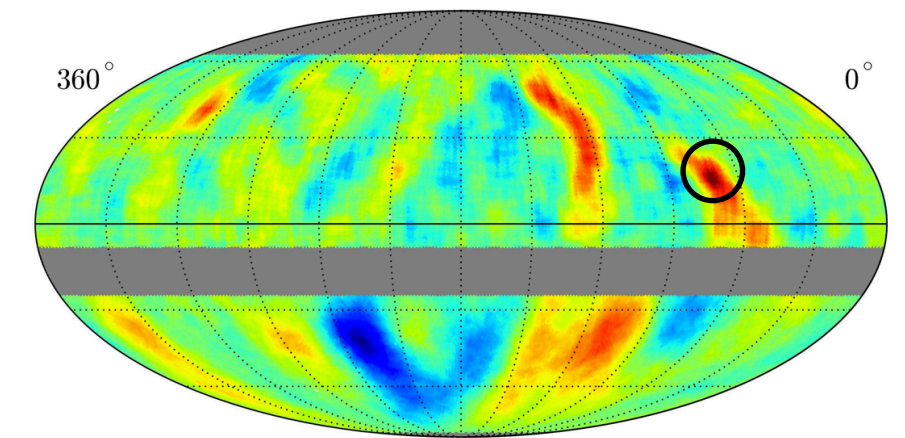
turbulent reconnection Lazarian & Vishniac 1999

1st order Fermi acceleration de Gouveia dal Pino & Lazarian 2003, 2005

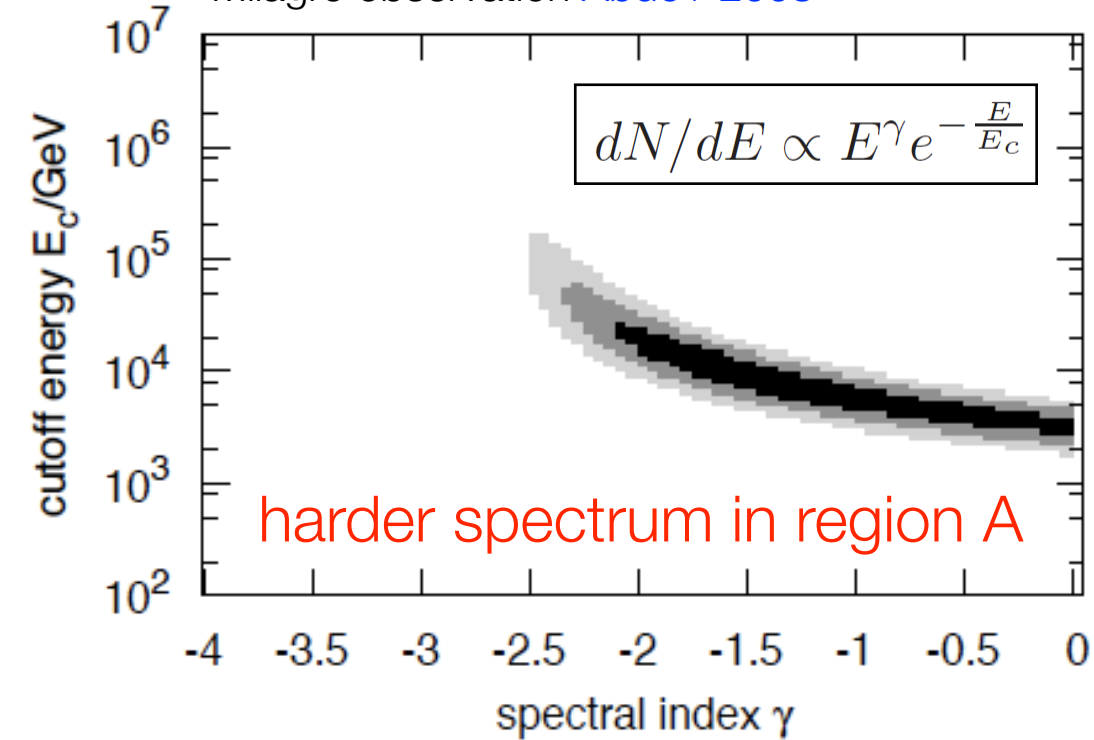
$$E_{max} \approx 0.5 \left(\frac{B}{1 \mu G} \right) \left(\frac{L_{zone}}{100 AU} \right) TeV \approx 0.5 - 6 TeV$$

Lazarian, PD 2010 - PD, Lazarian 2012

► detailed modeling of heliotail very important

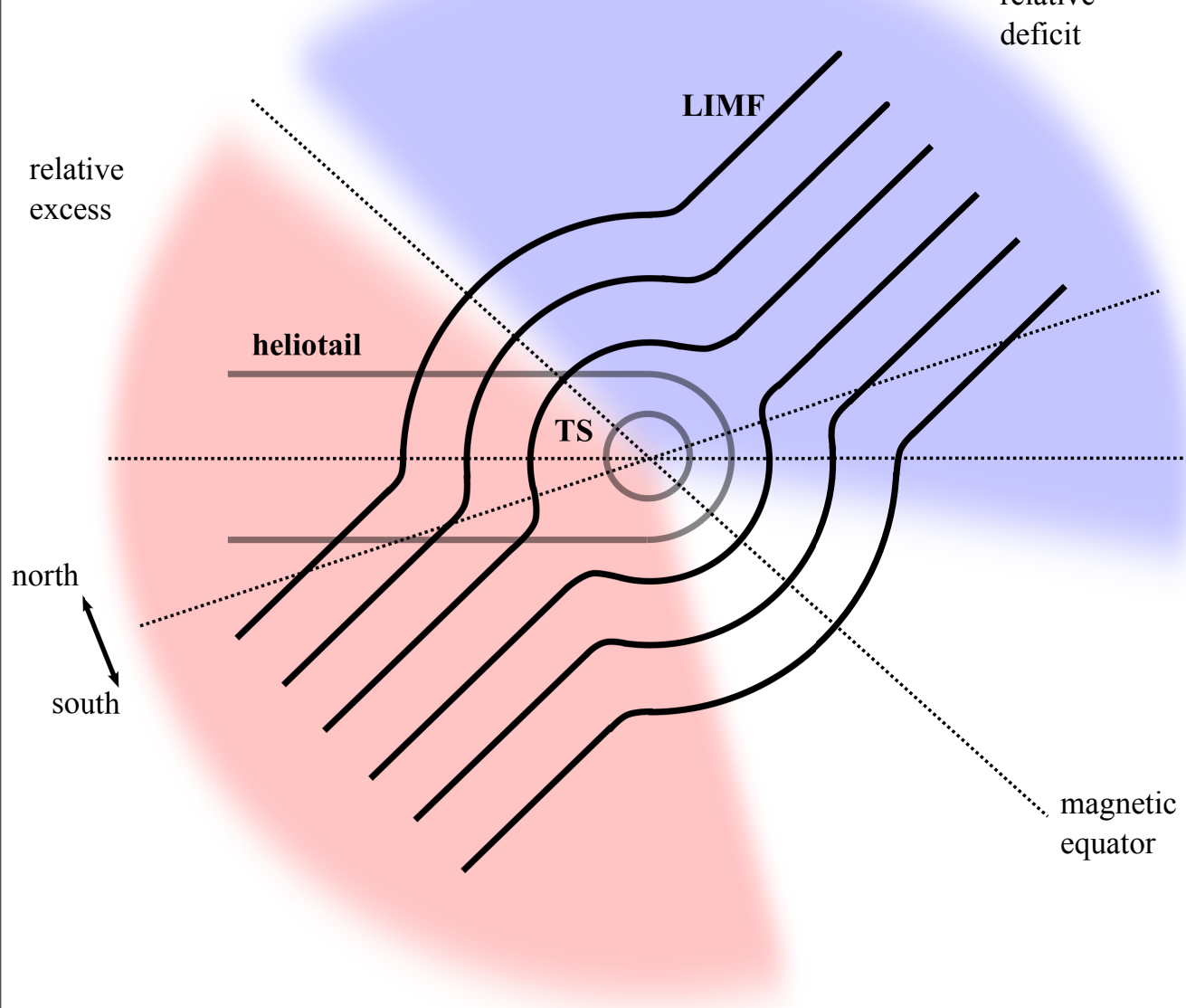


Milagro observation Abdo+ 2008

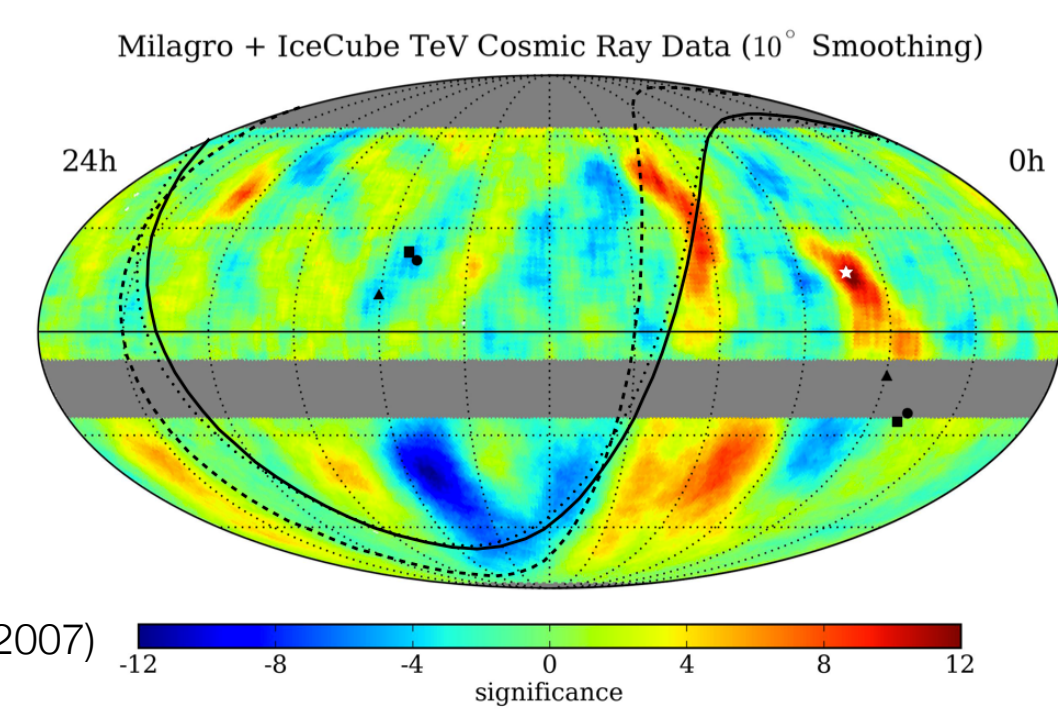
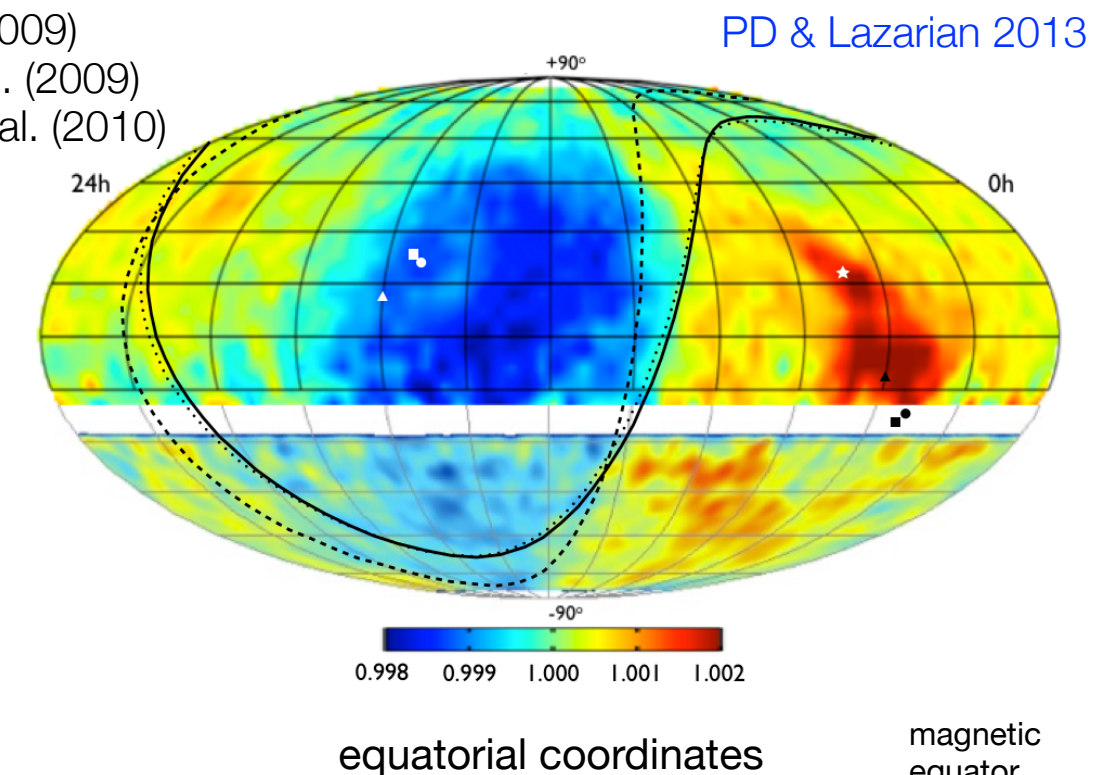


$\gamma < \gamma_{elsewhere}$ at 4.6 σ level
 $E_c = 3 - 25$ TeV

cosmic ray anisotropy & scattering heliospheric perturbations



Funsten et al. (2009)
Schwadron et al. (2009)
Heerikhuisen et al. (2010)

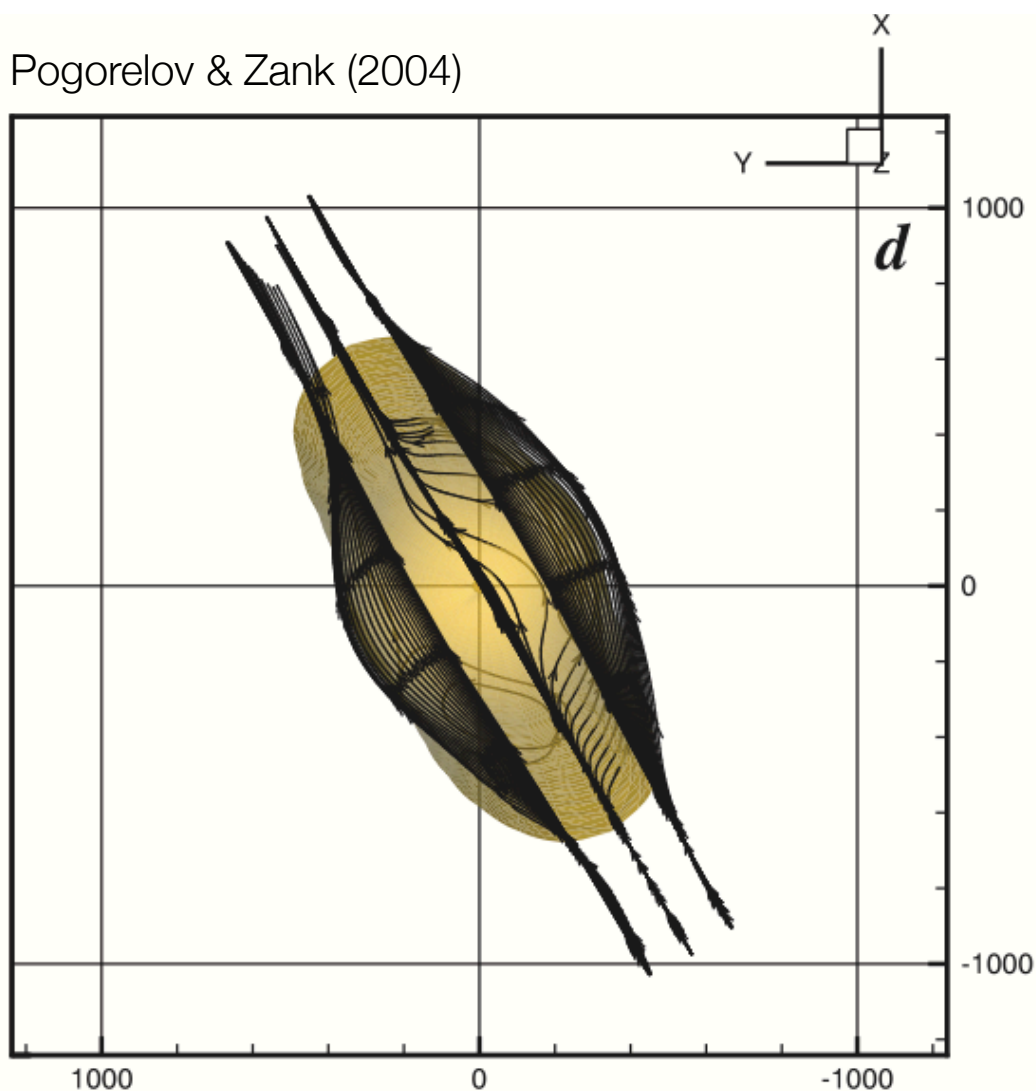


LIMF direction compatible with

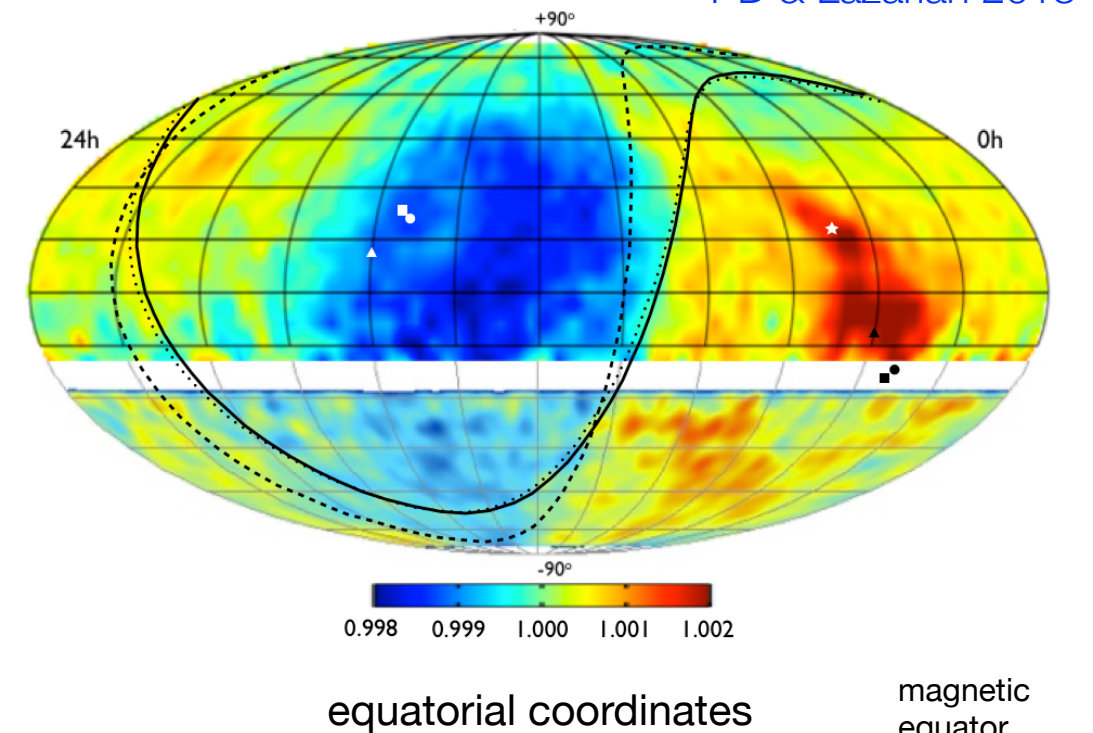
- Ca II absorption & H I lines, Frisch (1996)
- radio emission from inner heliosheath, Lallement et al. (2005), Opher et al. (2007)
- polarization measurements, Frisch (2010)

cosmic ray anisotropy & scattering heliospheric perturbations

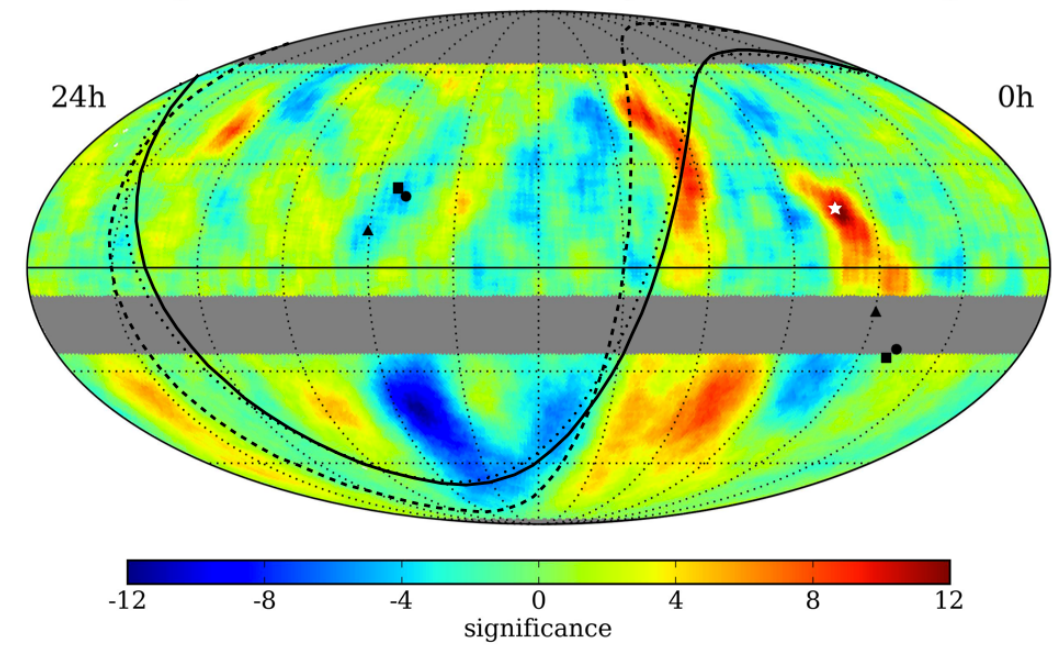
Pogorelov & Zank (2004)



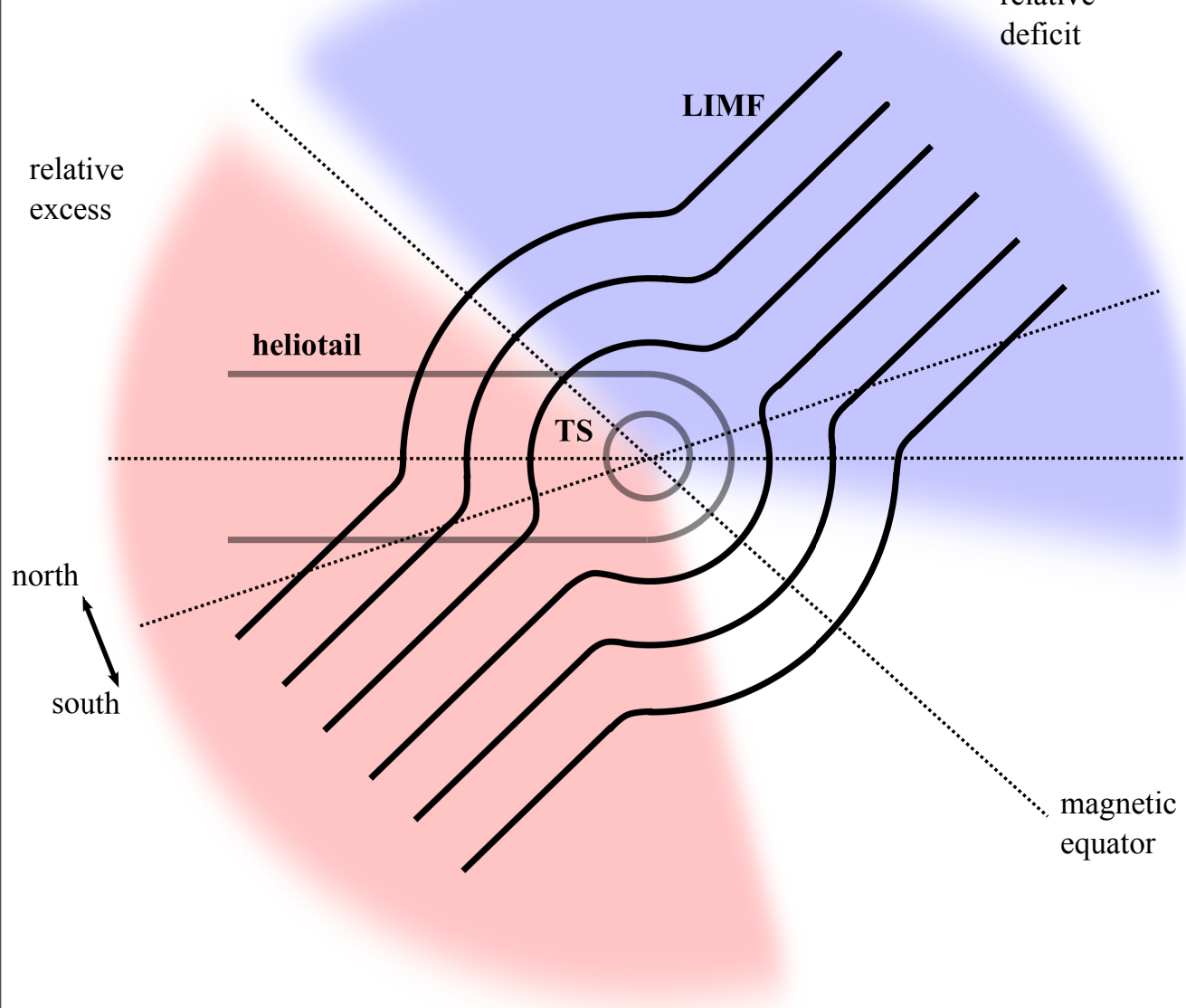
PD & Lazarian 2013



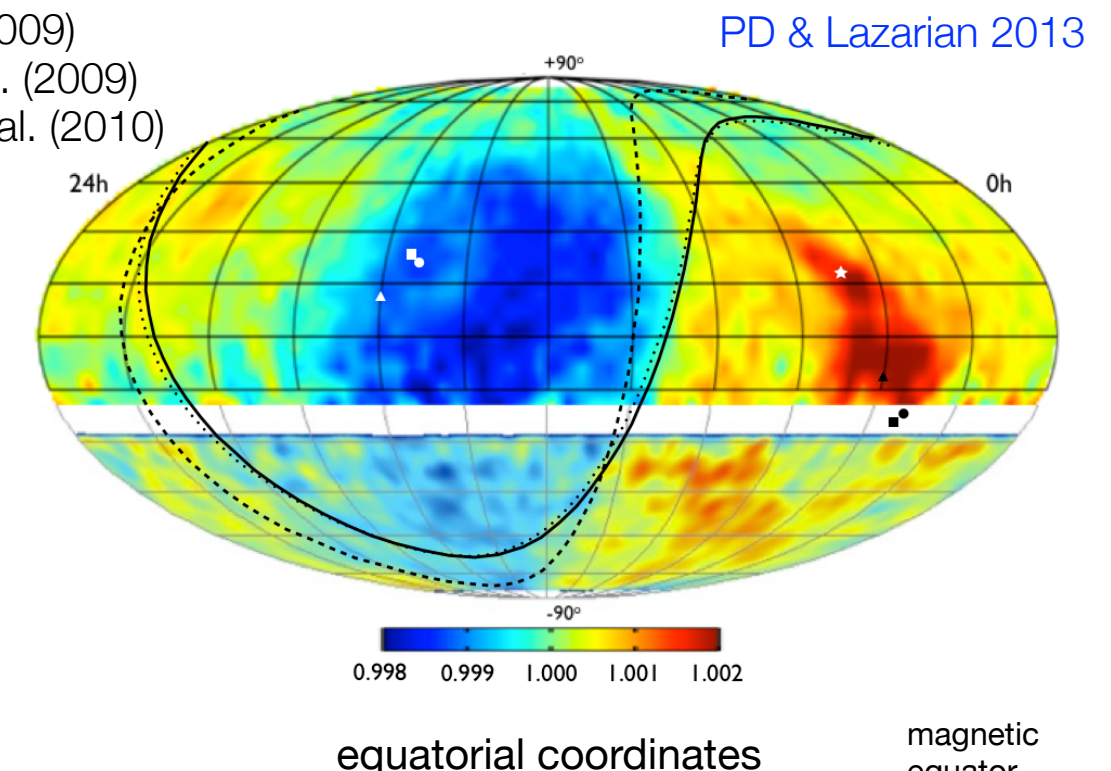
Milagro + IceCube TeV Cosmic Ray Data (10° Smoothing)



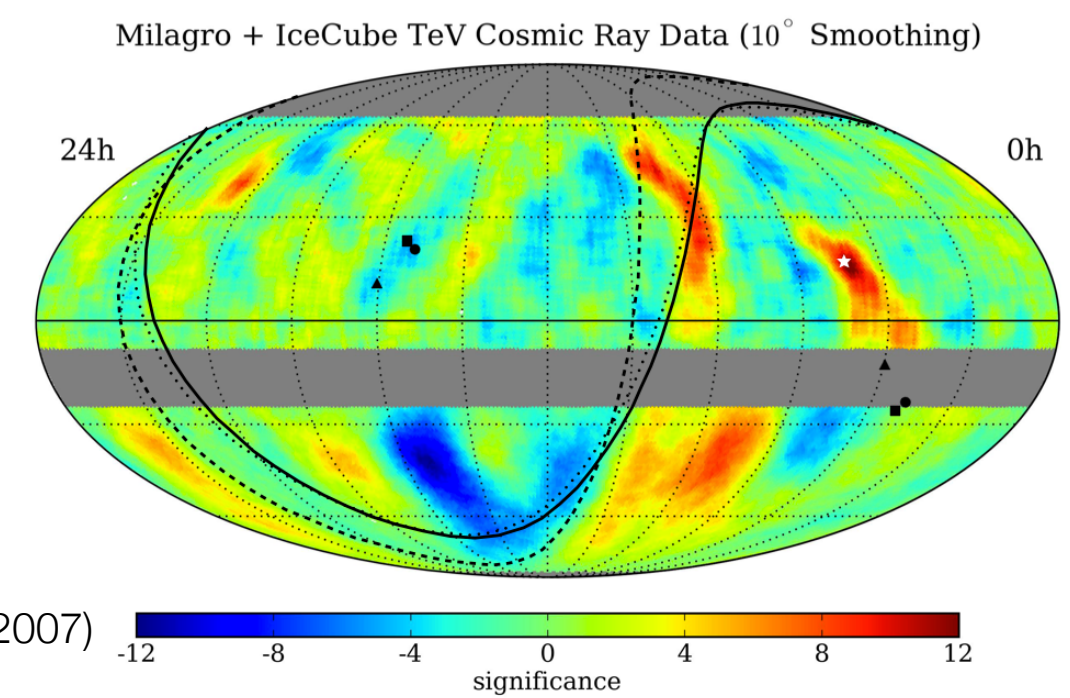
cosmic ray anisotropy & scattering heliospheric perturbations



Funsten et al. (2009)
Schwadron et al. (2009)
Heerikhuisen et al. (2010)

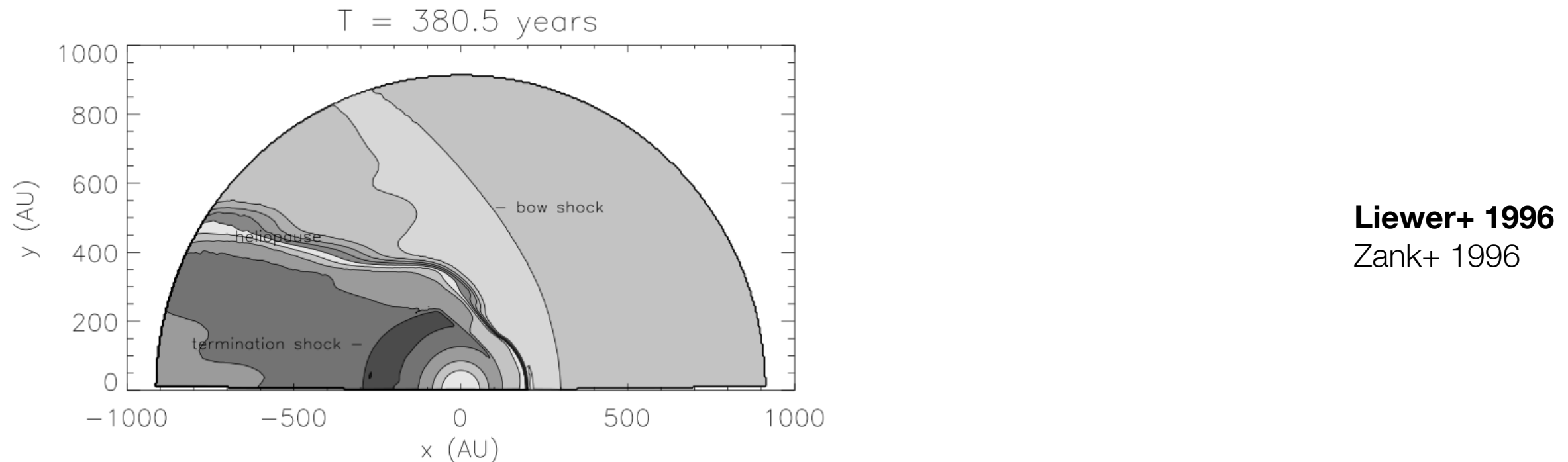


- LIMF direction compatible with
- Ca II absorption & H I lines, Frisch (1996)
 - radio emission from inner heliosheath, Lallement et al. (2005), Opher et al. (2007)
 - polarization measurements, Frisch (2010)

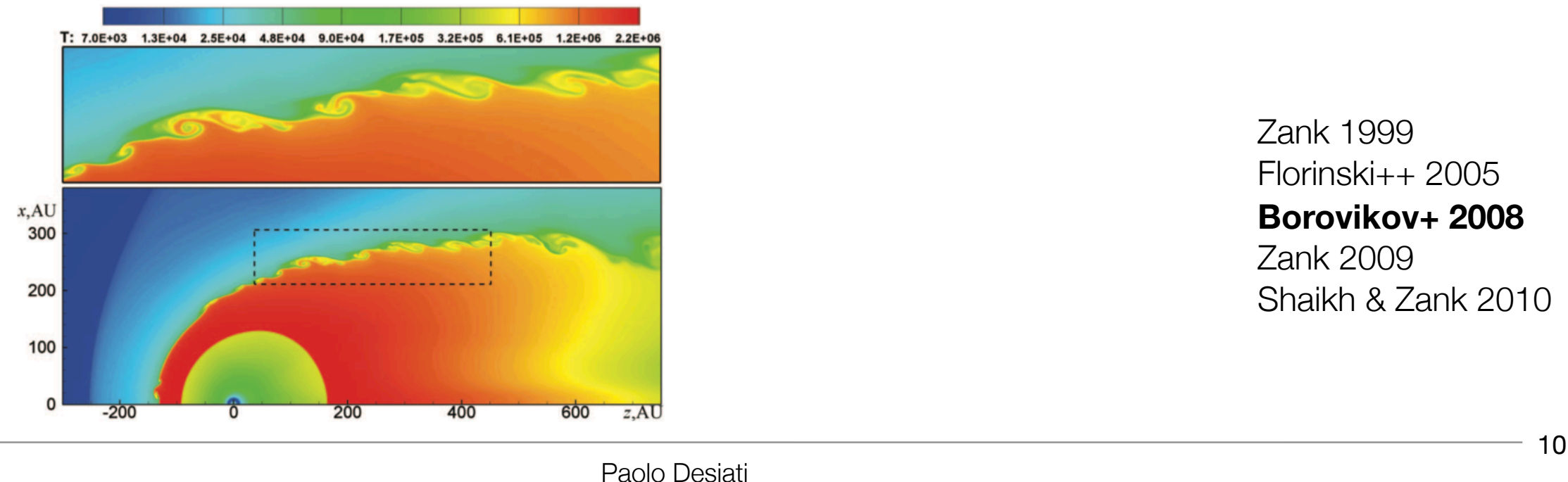


heliospheric perturbations instabilities

- Rayleigh-Taylor instabilities driven and mediated by interstellar neutral atoms

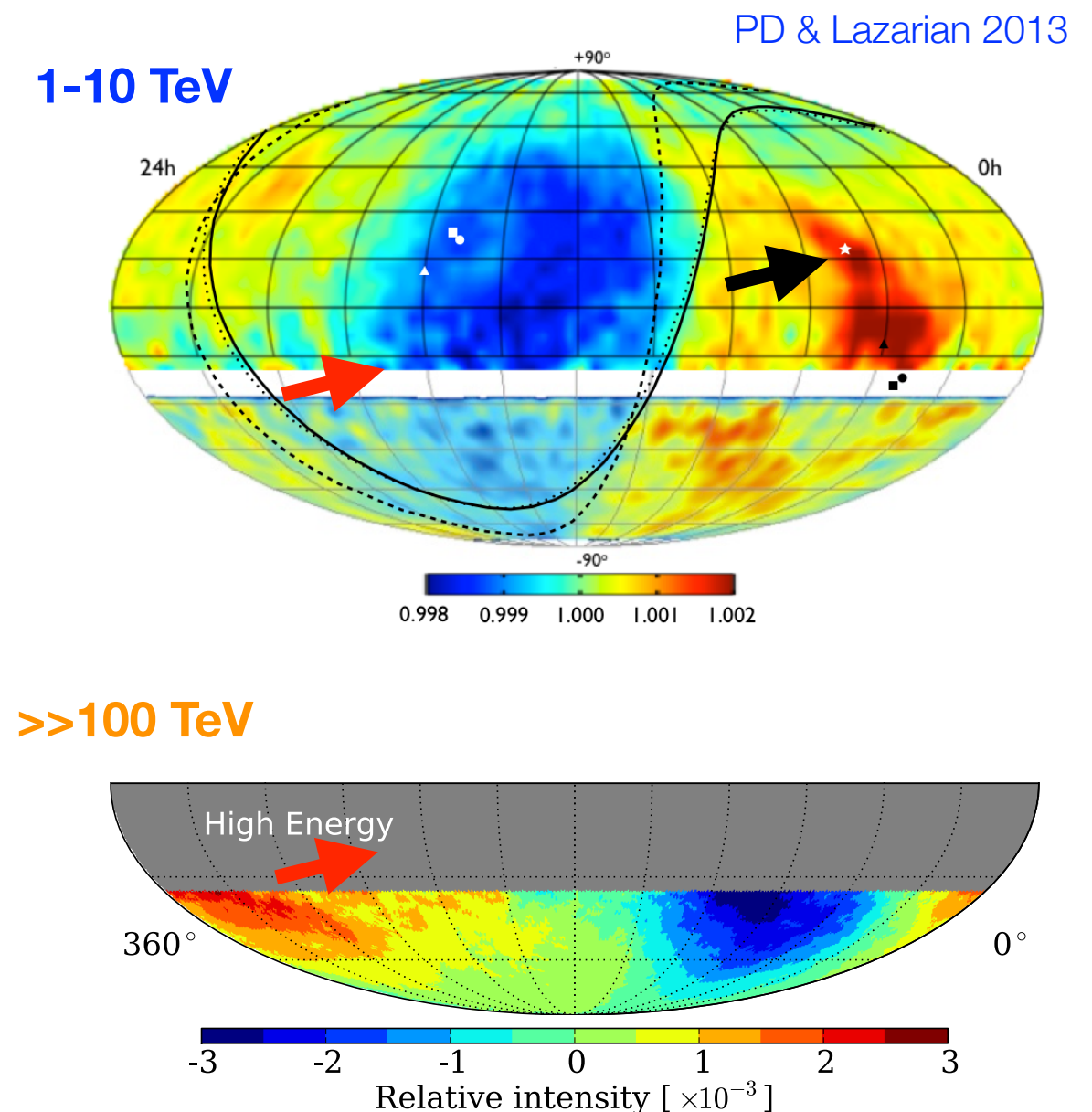
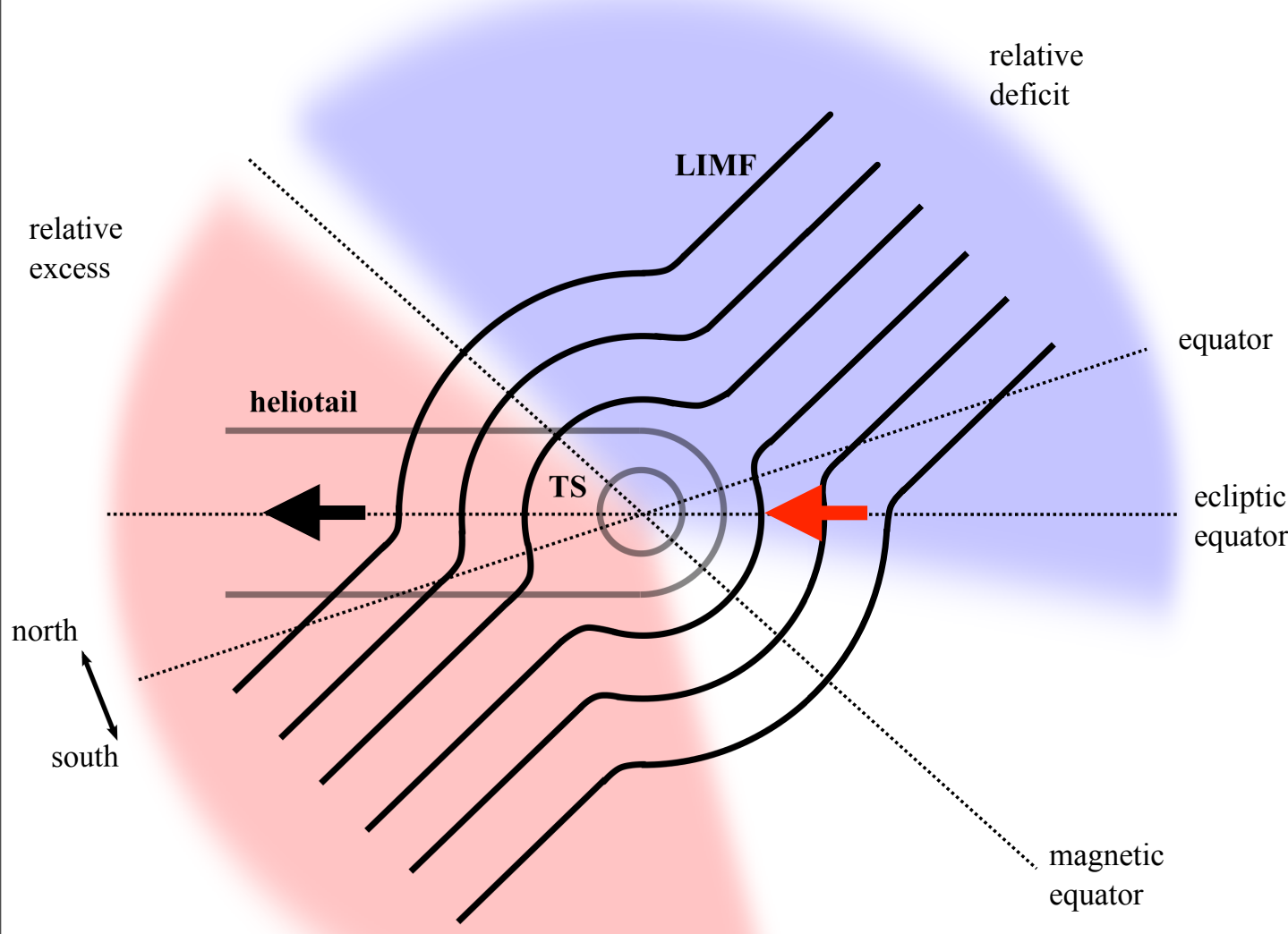


- plasma-fluid instabilities at the flank of HP by charge exchange processes



cosmic ray anisotropy

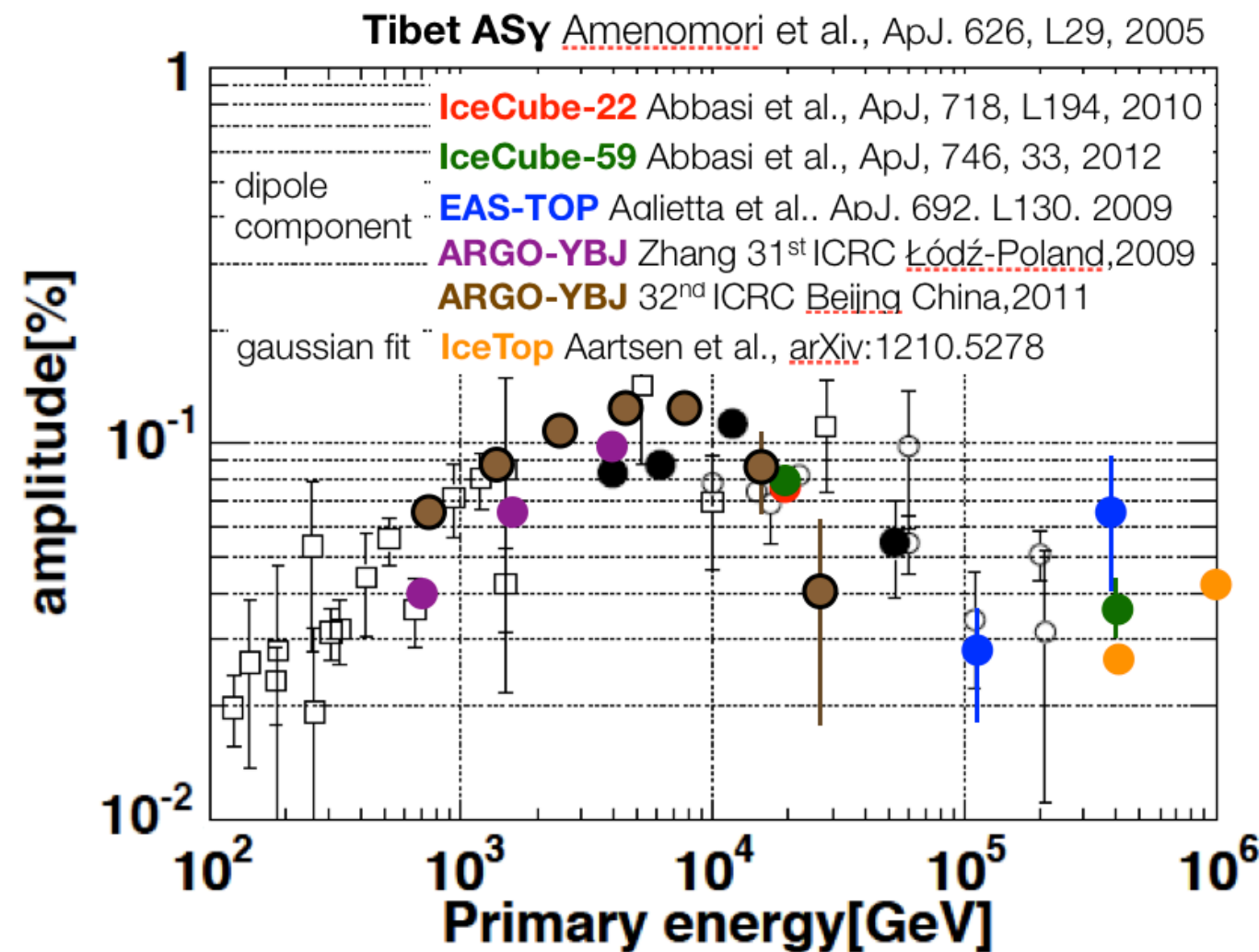
influence of perturbed heliotail



anisotropy re-directed due to scattering on magnetic perturbations on the heliospheric boundary

scattering on heliospheric boundary toy model

- @ energy scale of 10 TeV - proton resonant scattering with perturbations at largest scale - scrambling of cosmic ray arrival directions

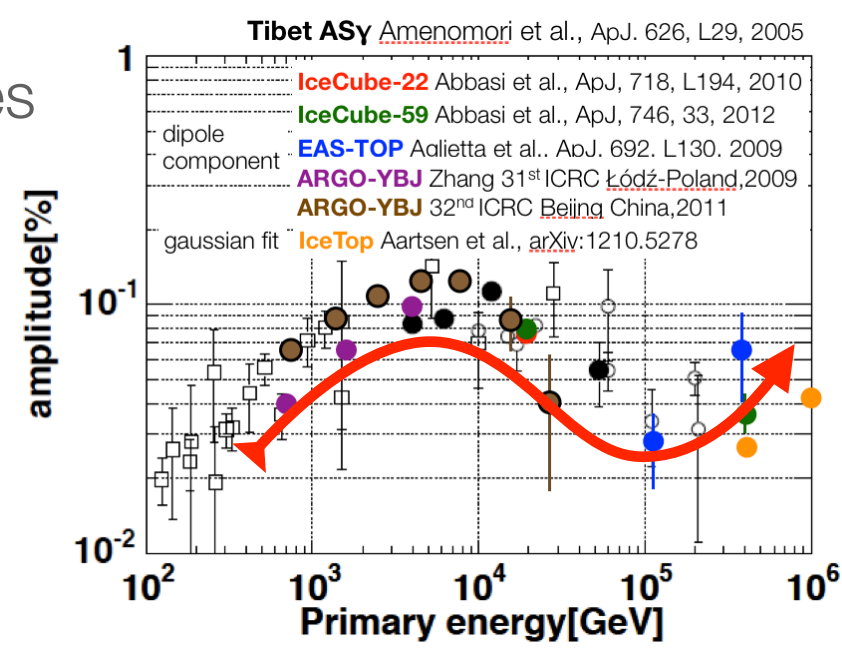


scattering on heliospheric boundary toy model

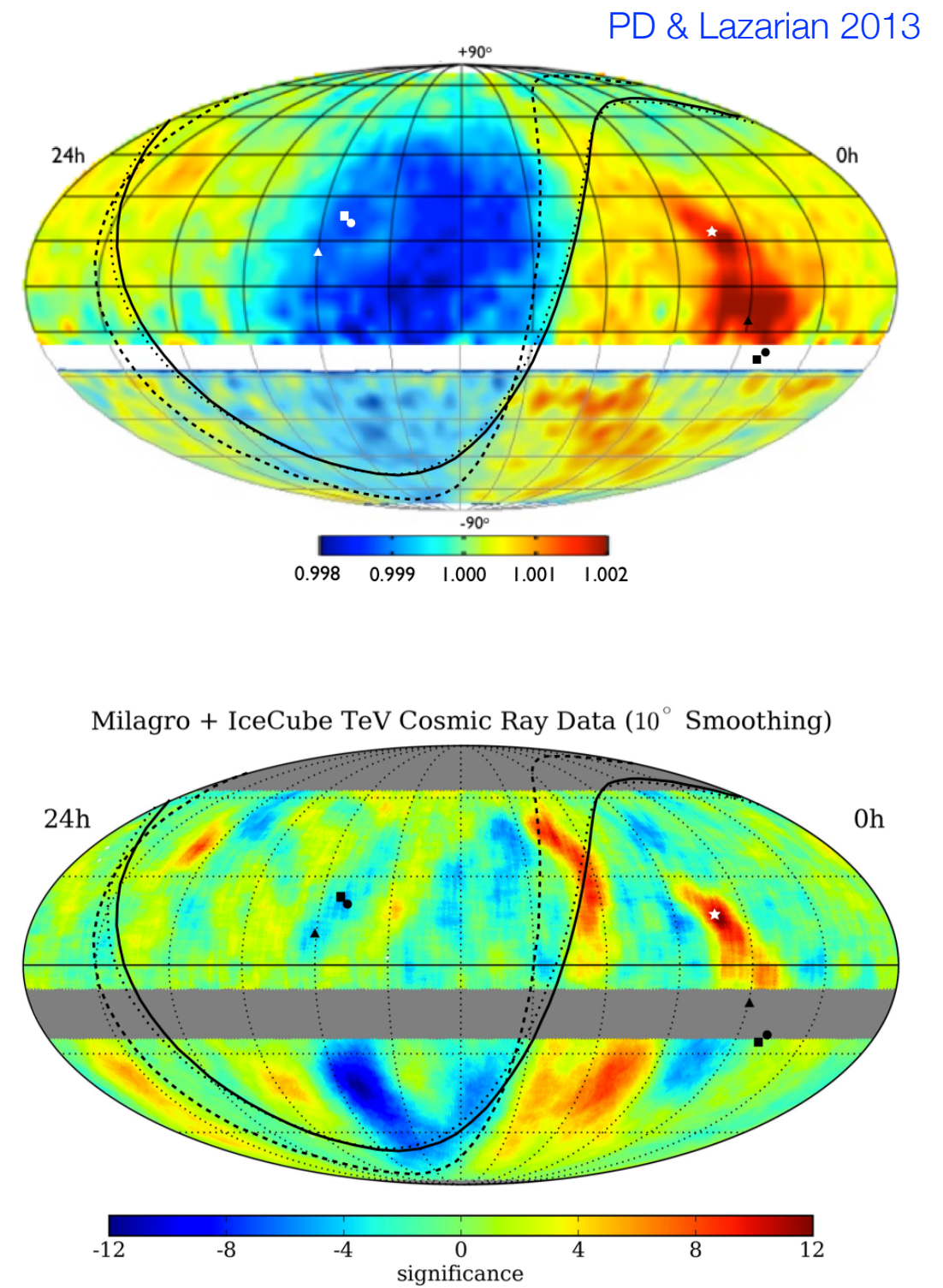
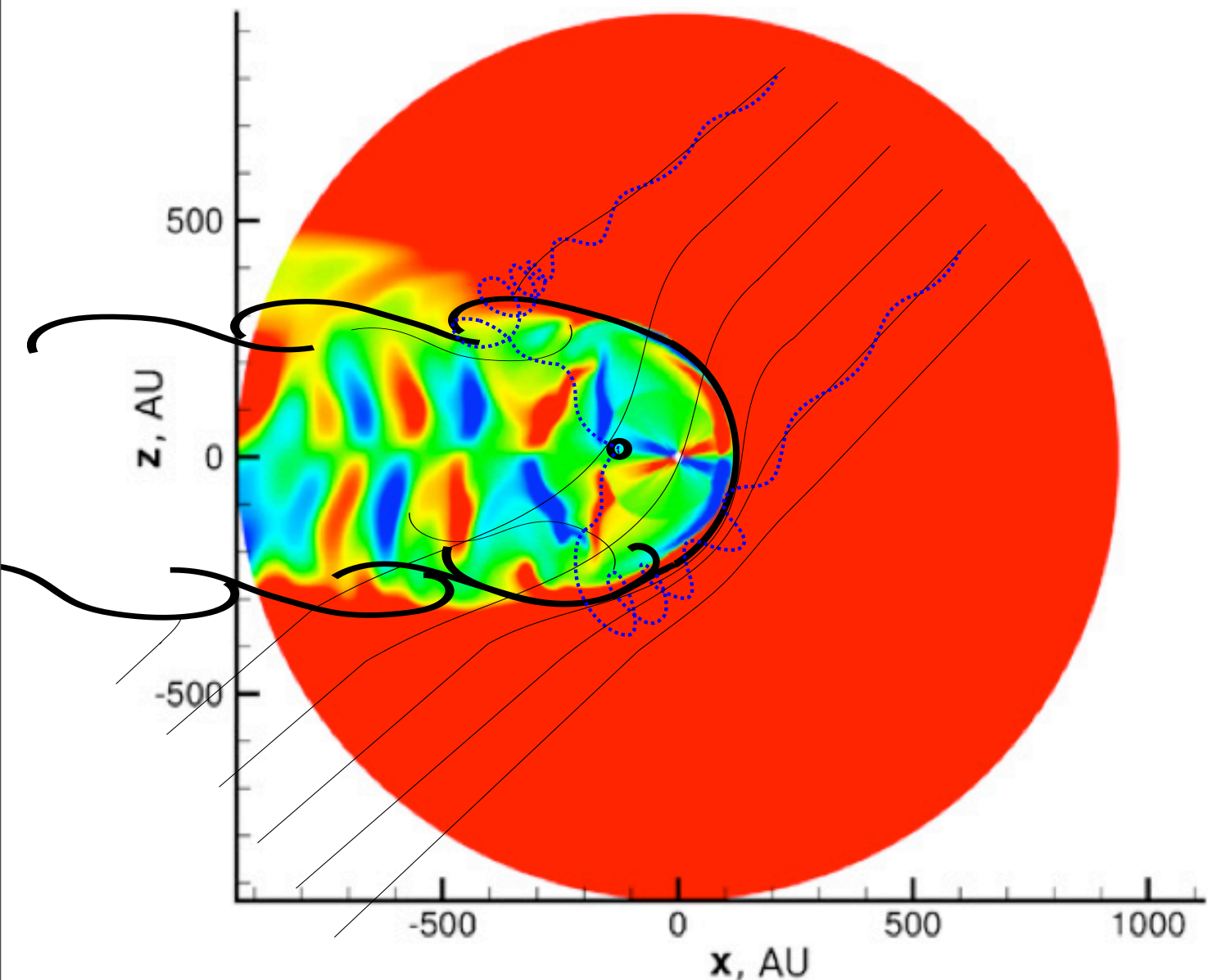
- @ energy scale of 10 TeV - proton resonant scattering with perturbations at largest scale - scrambling of cosmic ray arrival directions
- < 10 TeV - resonant scattering with smaller scale perturbations - pitch angle variations from p^2_{\perp}/B at larger scale
- > 10 TeV - non-resonant scattering with smaller scales - amplitude decreases, intensity gradient become smoother
- > 100 TeV - $r_L >$ heliosphere - heliospheric influence dissipates

► CR mass composition - smearing of transition scale

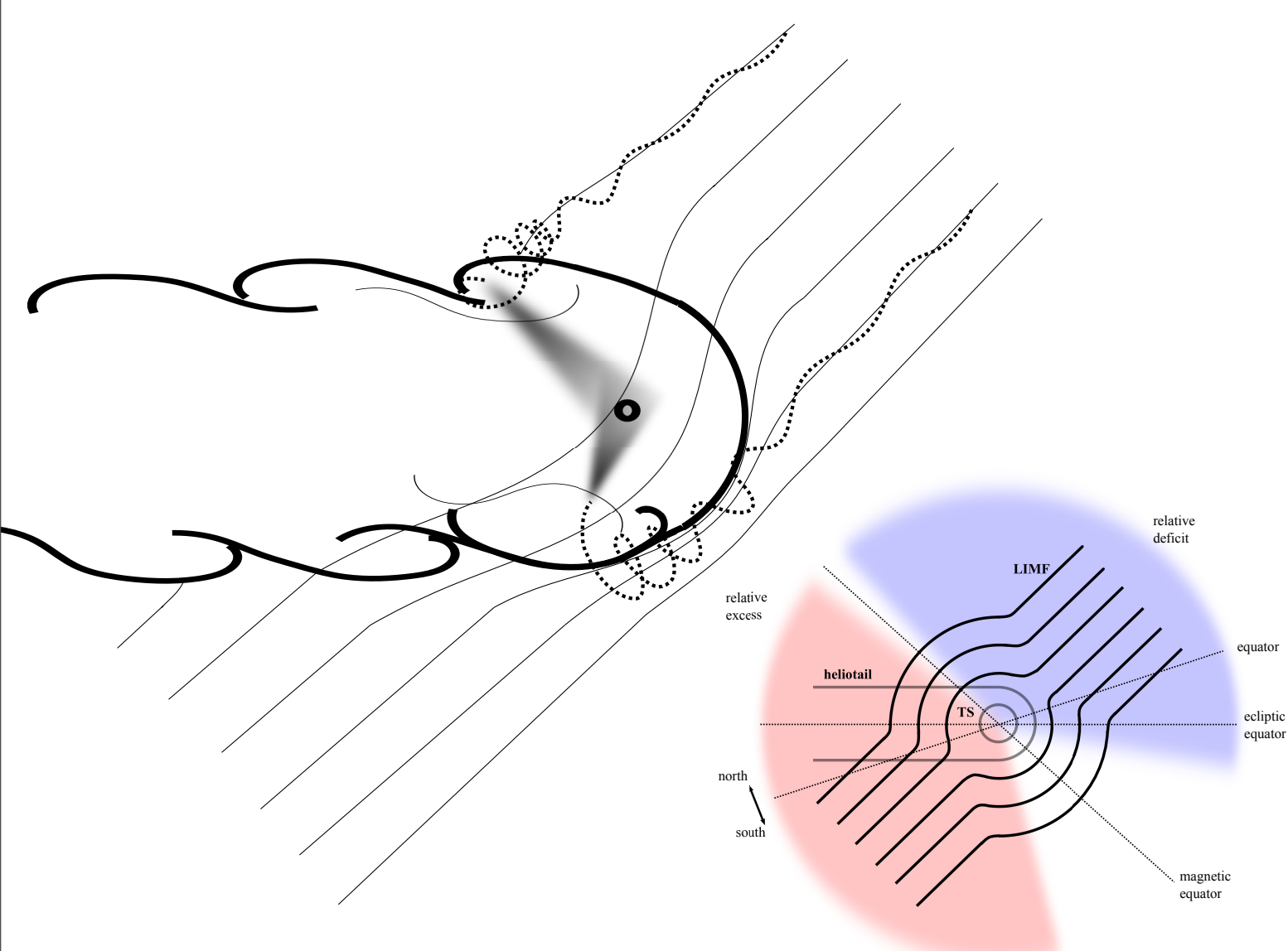
► re-directed anisotropy not a dipole



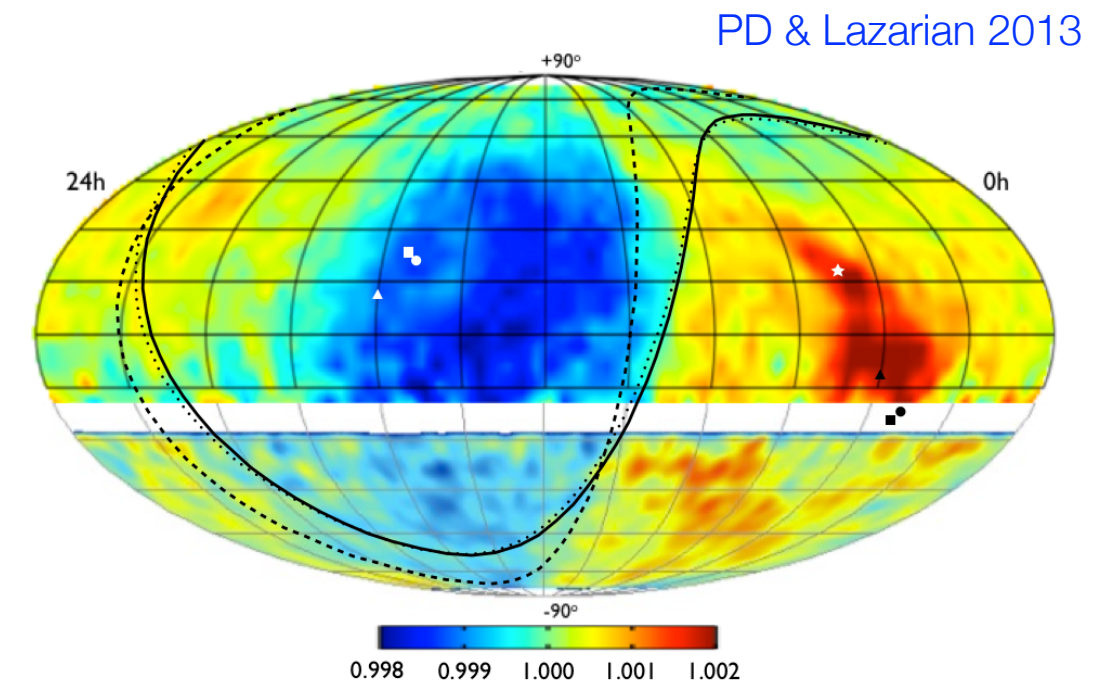
scattering on heliospheric boundary toy model



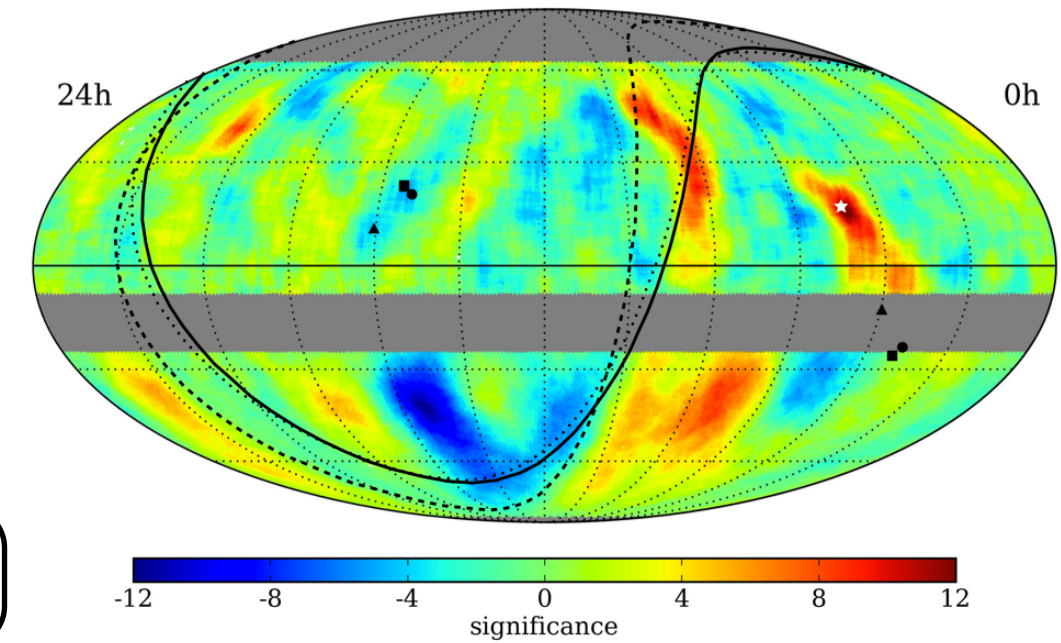
scattering on heliospheric boundary toy model



► detailed modeling of heliotail very important



Milagro + IceCube TeV Cosmic Ray Data (10° Smoothing)

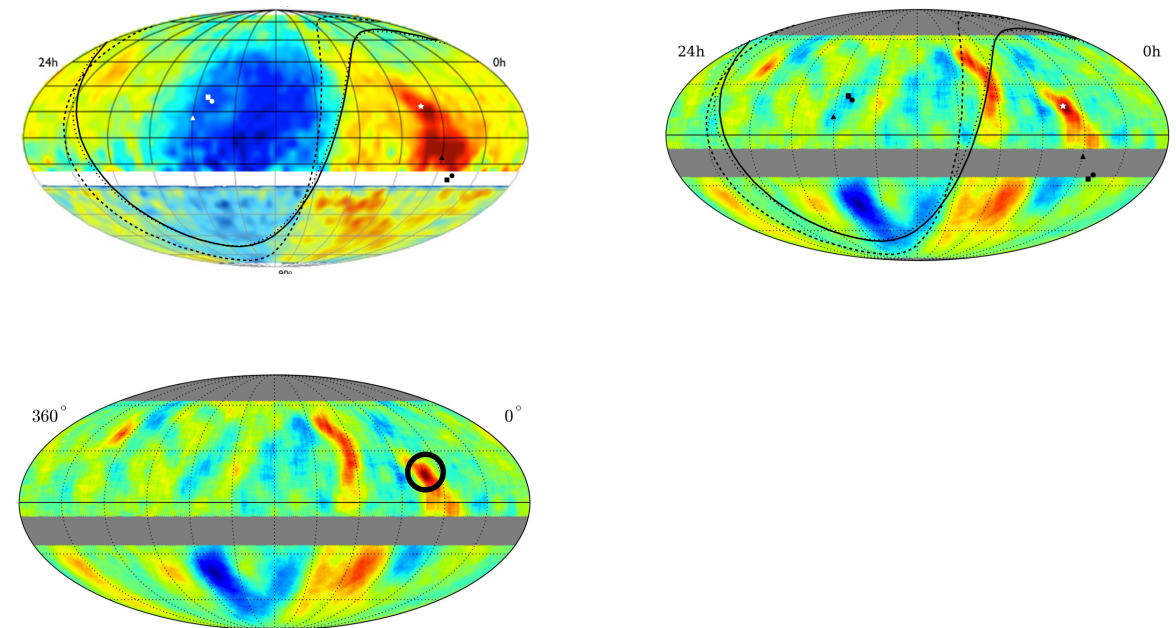


conclusions

- high energy **cosmic ray anisotropy** to probe into their **origin** and **propagation**
- astrophysical scenarios need understanding of local phenomena
- <100 TeV cosmic rays to be affected by heliosphere
- **scattering** with perturbation on heliopause

- **re-acceleration** mechanism from heliotail

► heliospheric modeling to be extended along **heliotail** with fine resolution: turbulence & global structure. Particle trajectory integration studies will follow → predictive model

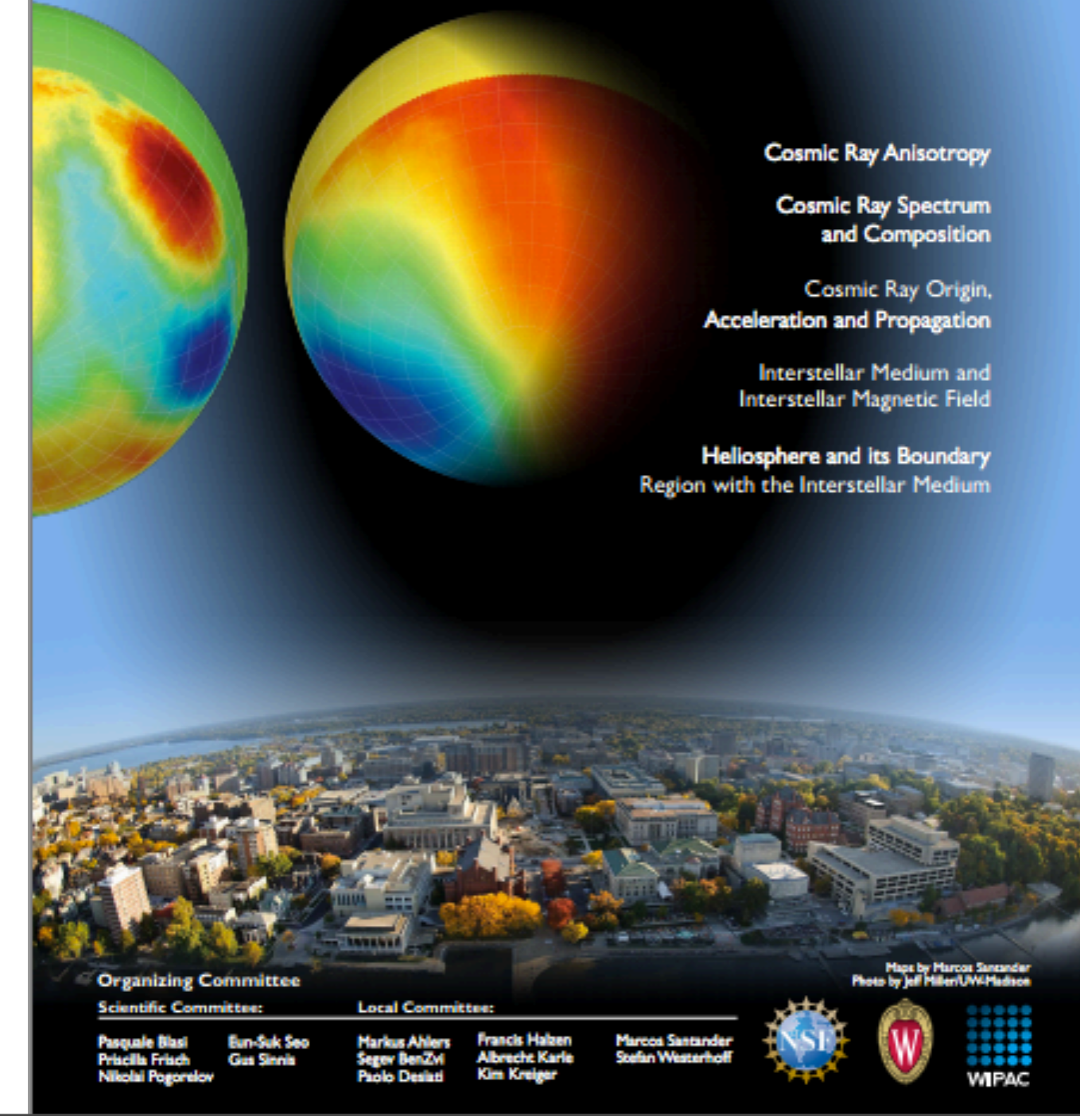


thank you

2013 Cosmic Ray Anisotropy Workshop

September 26-28, 2013

Union South • 1308W Dayton St • Madison, WI
wipac.wisc.edu/CRA2013



The image features a composite background. At the top, there are two scientific plots: a green sphere showing a central red/orange region and a larger yellow sphere showing a gradient from blue at the bottom to red at the top. Below these plots is a photograph of the University of Wisconsin-Madison campus, showing buildings and trees. In the bottom right corner, there is a small text note: "Host by Marcos Santander Photo by Jeff Miller/UW-Madison".

Cosmic Ray Anisotropy

Cosmic Ray Spectrum and Composition

Cosmic Ray Origin, Acceleration and Propagation

Interstellar Medium and Interstellar Magnetic Field

Heliopause and its Boundary Region with the Interstellar Medium

Organizing Committee

Scientific Committee:

Pasquale Blasi	Bun-Suk Seo	Markus Ahlers	Francis Halzen	Marcos Santander
Priscilla Frisch	Gus Sinnis	Segev BenZvi	Albrecht Karle	Stefan Westerhoff
Nikolai Pogorelov	Paolo Dordio	Paolo Dordio	Kim Kreiger	

Local Committee:

Francis Halzen	Albrecht Karle	Kim Kreiger
----------------	----------------	-------------

Host by Marcos Santander
Photo by Jeff Miller/UW-Madison

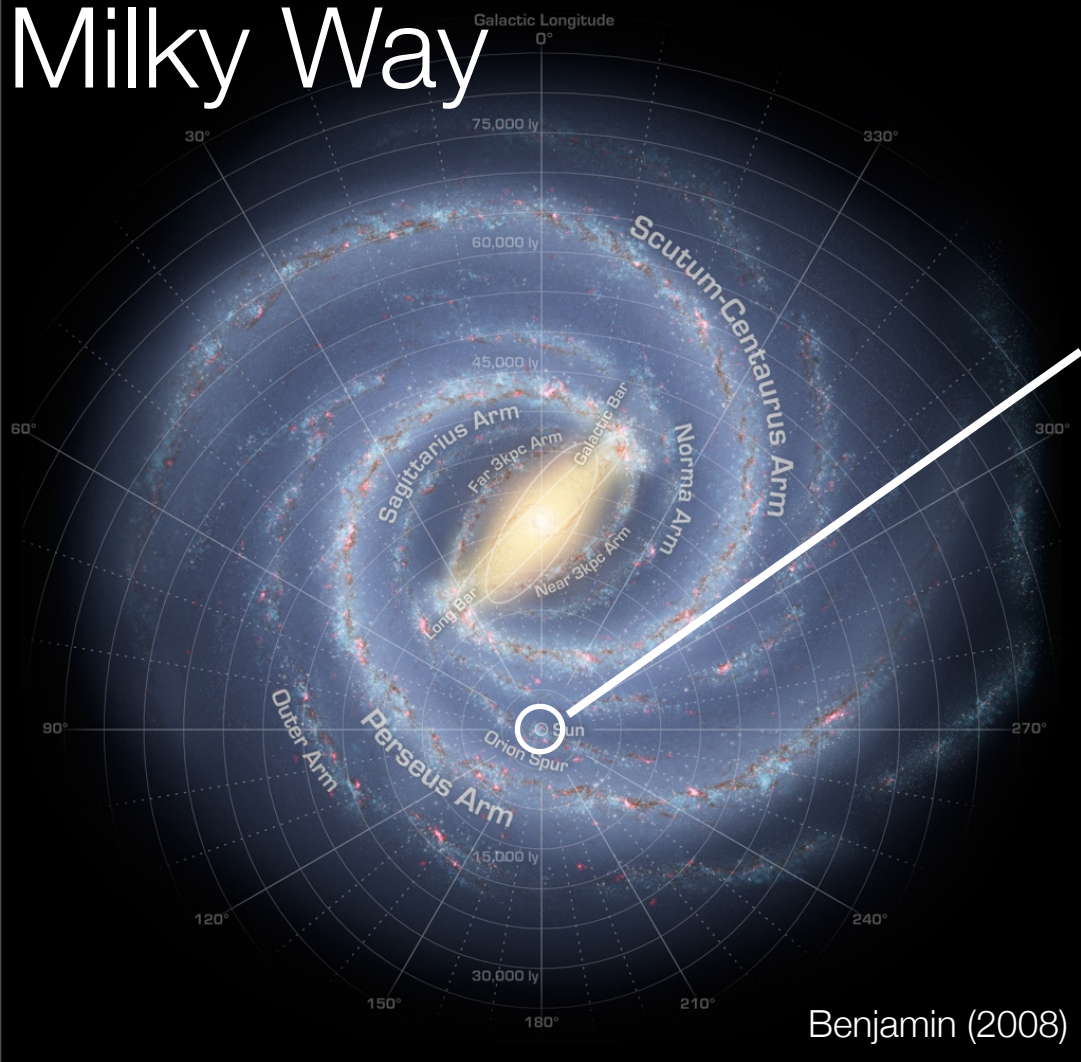
  

backup

$$R_g \approx \frac{200}{Z} \left(\frac{E}{1 \text{TeV}} \right) \left(\frac{\mu G}{B} \right) \text{AU}$$

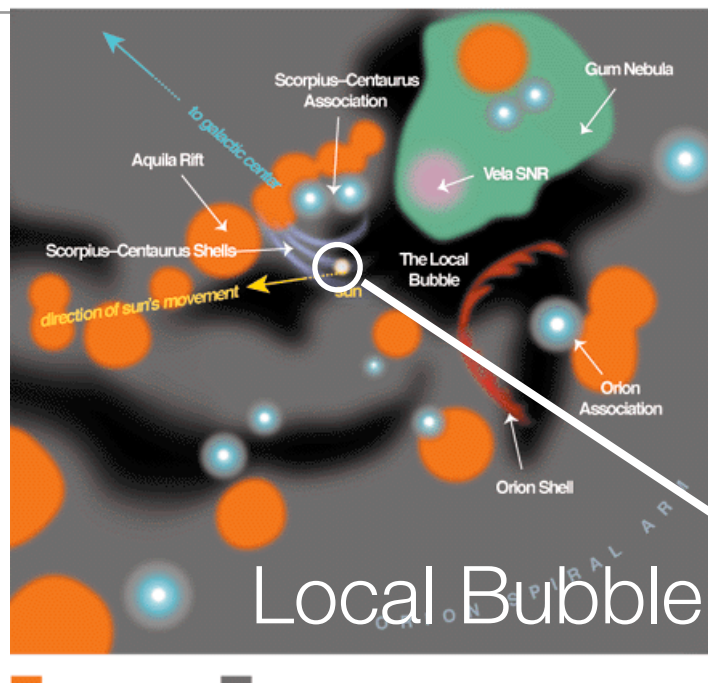
from the Galaxy to our local interstellar medium

Milky Way



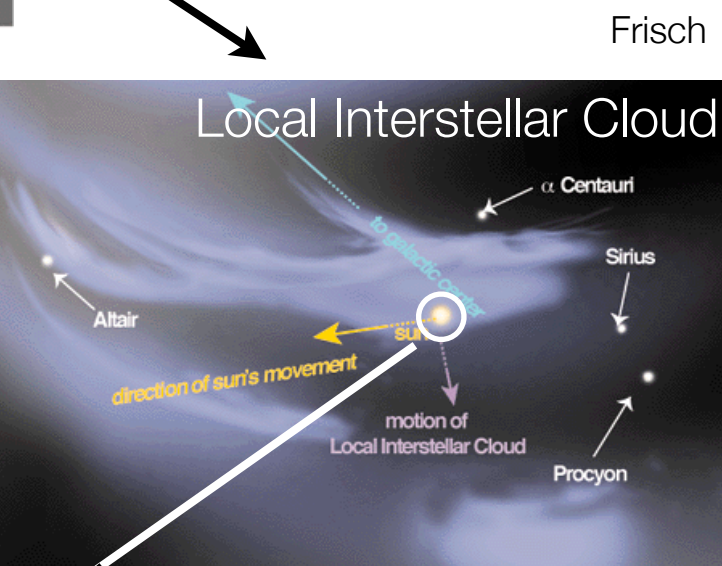
< 30,000 pc > (80 EeV)

(3 TeV - 140 TeV) < 200 AU - 10^4 AU >

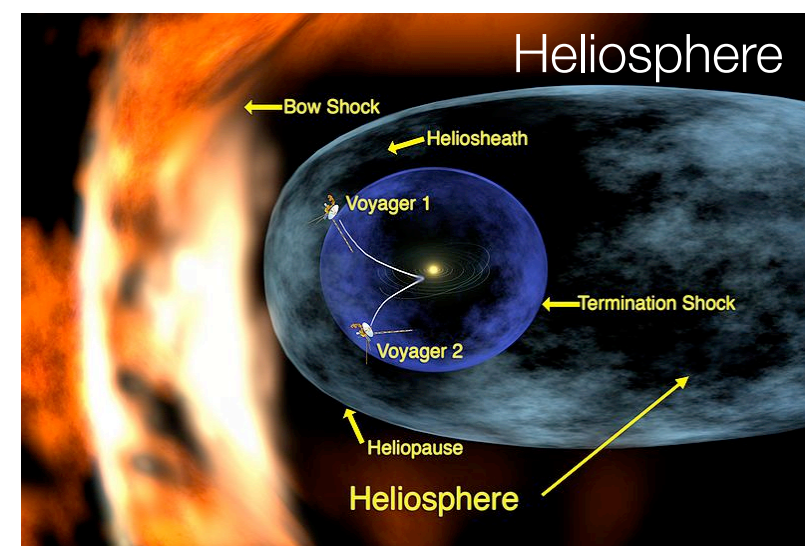


< 500 pc > (1.4 EeV)

Frisch

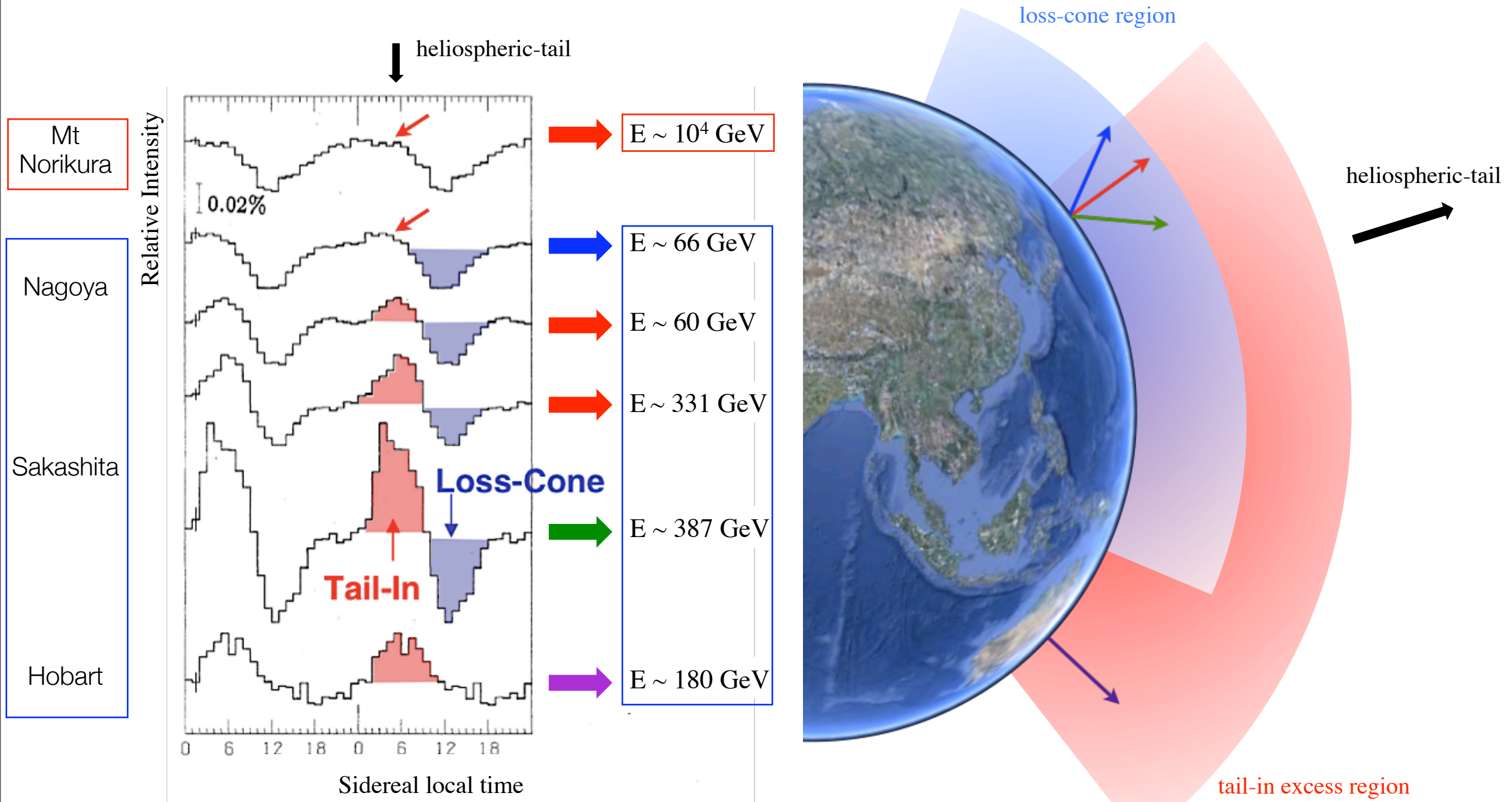


< 10-50 pc >
(30 PeV - 140 PeV)

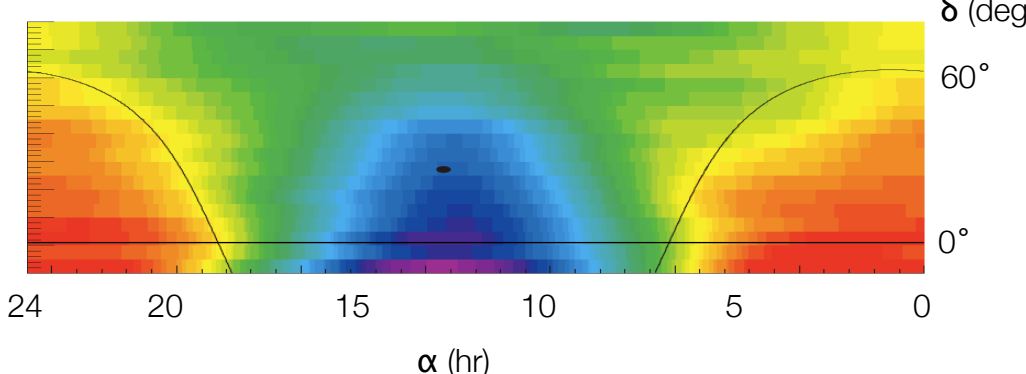
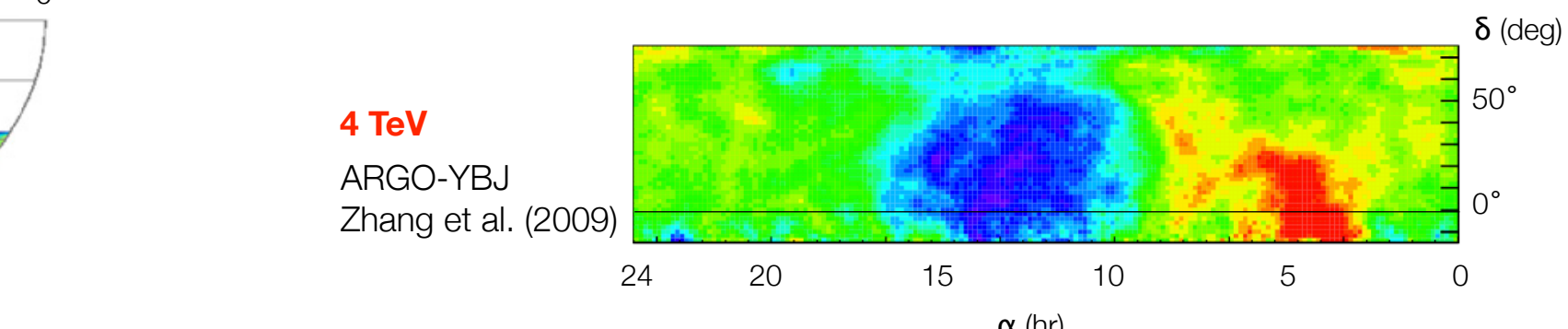
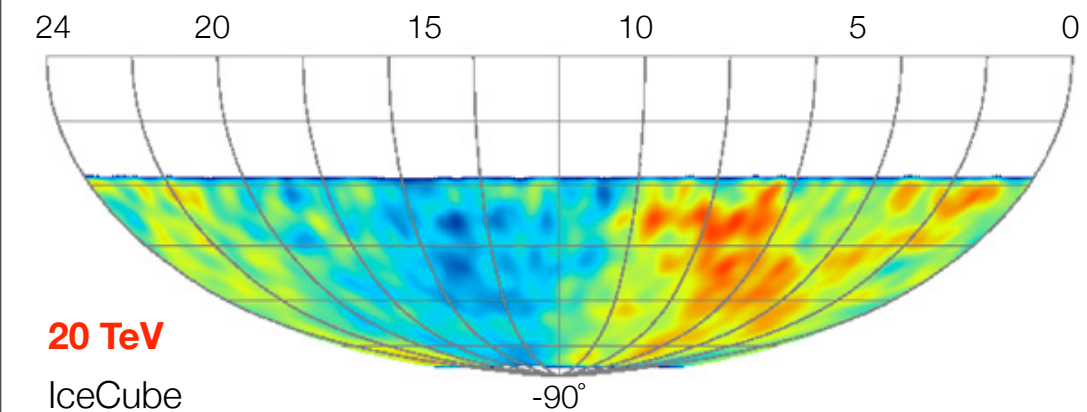
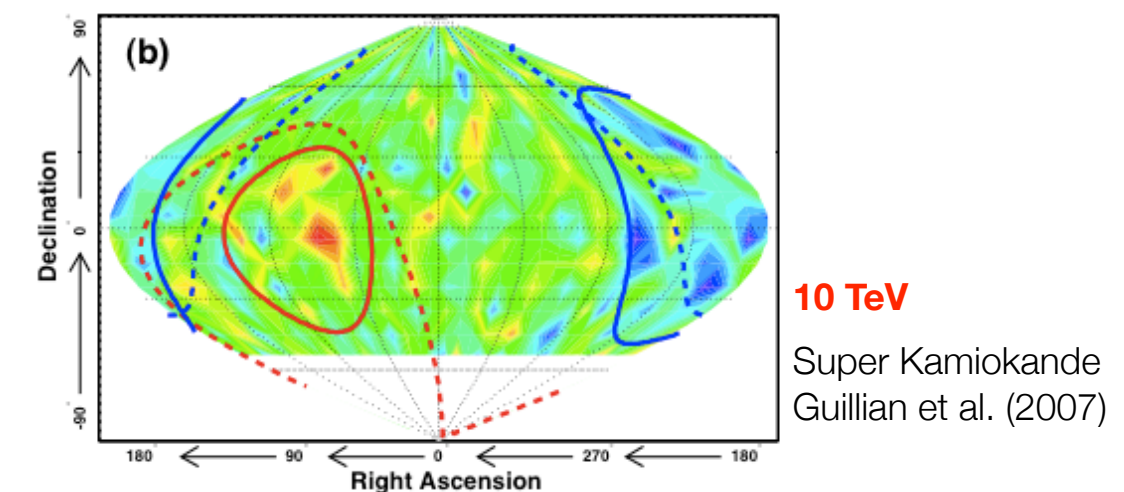
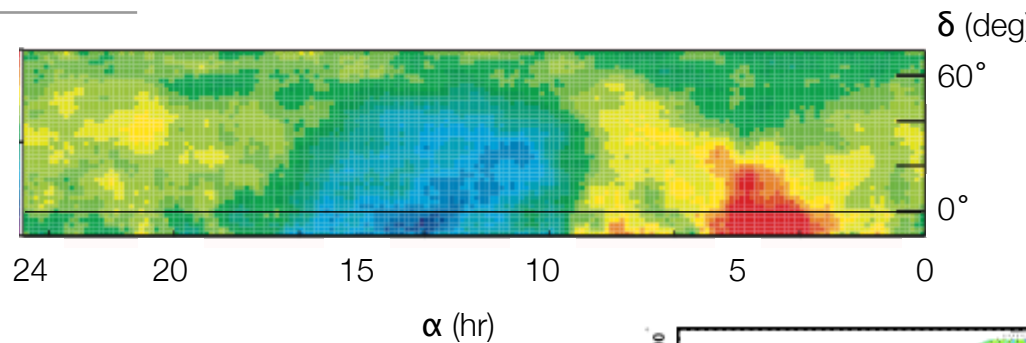
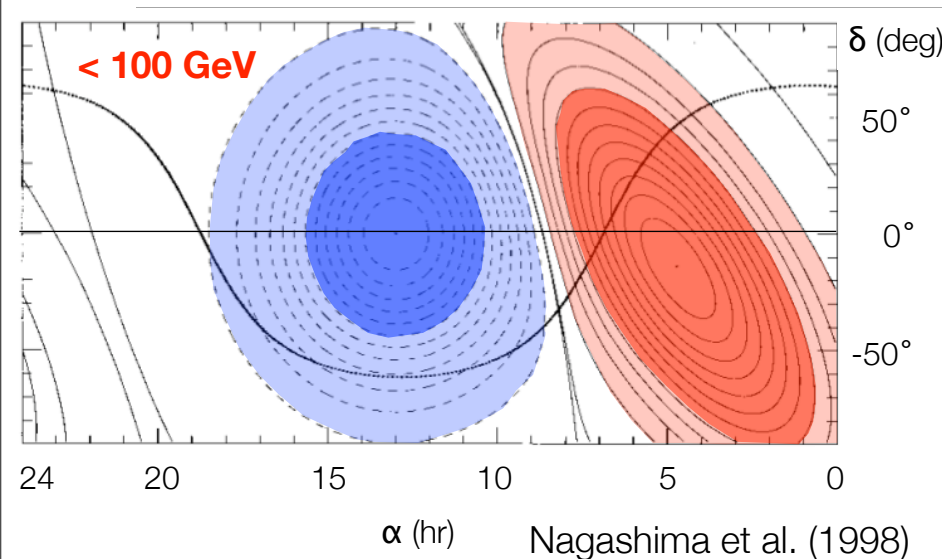
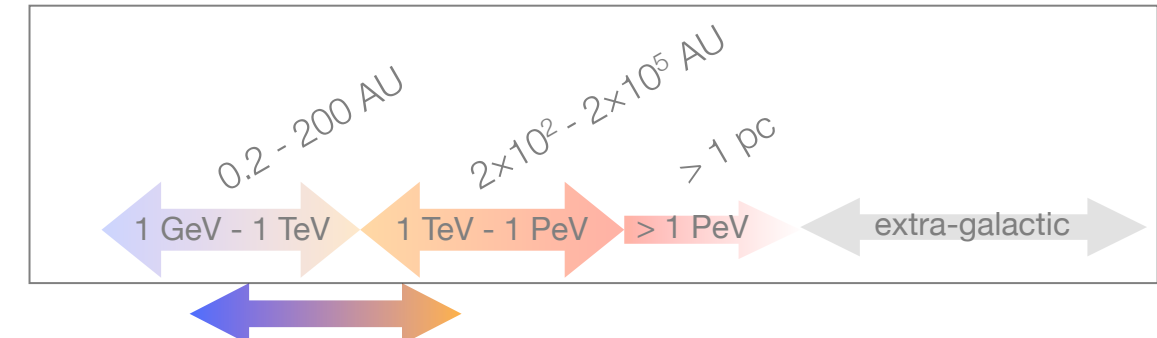


low energy cosmic ray anisotropy in arrival direction

Nagashima et al., J. Geophys. Res., Vol 103, No. A8, Pag. 17,429 (1998)

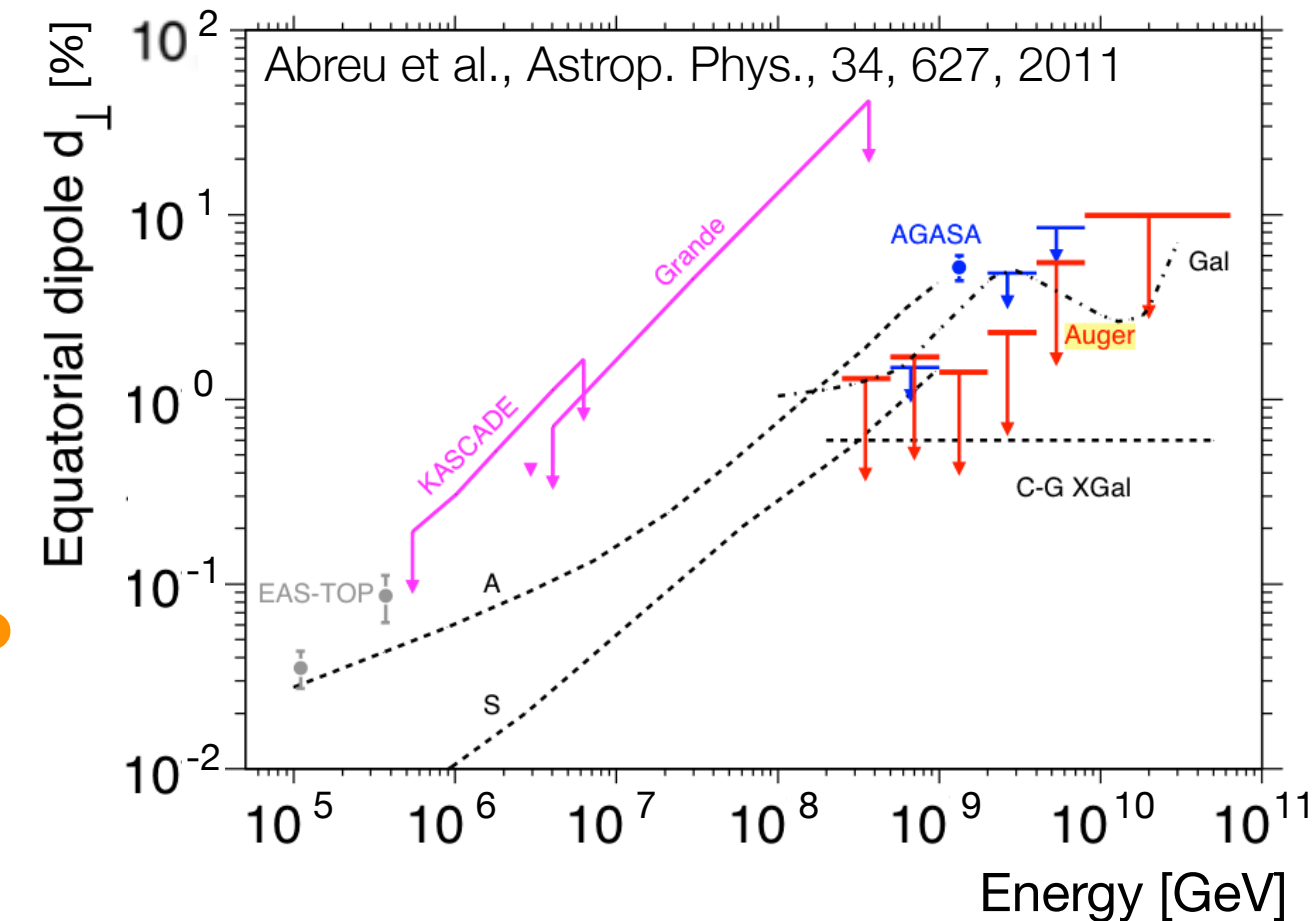
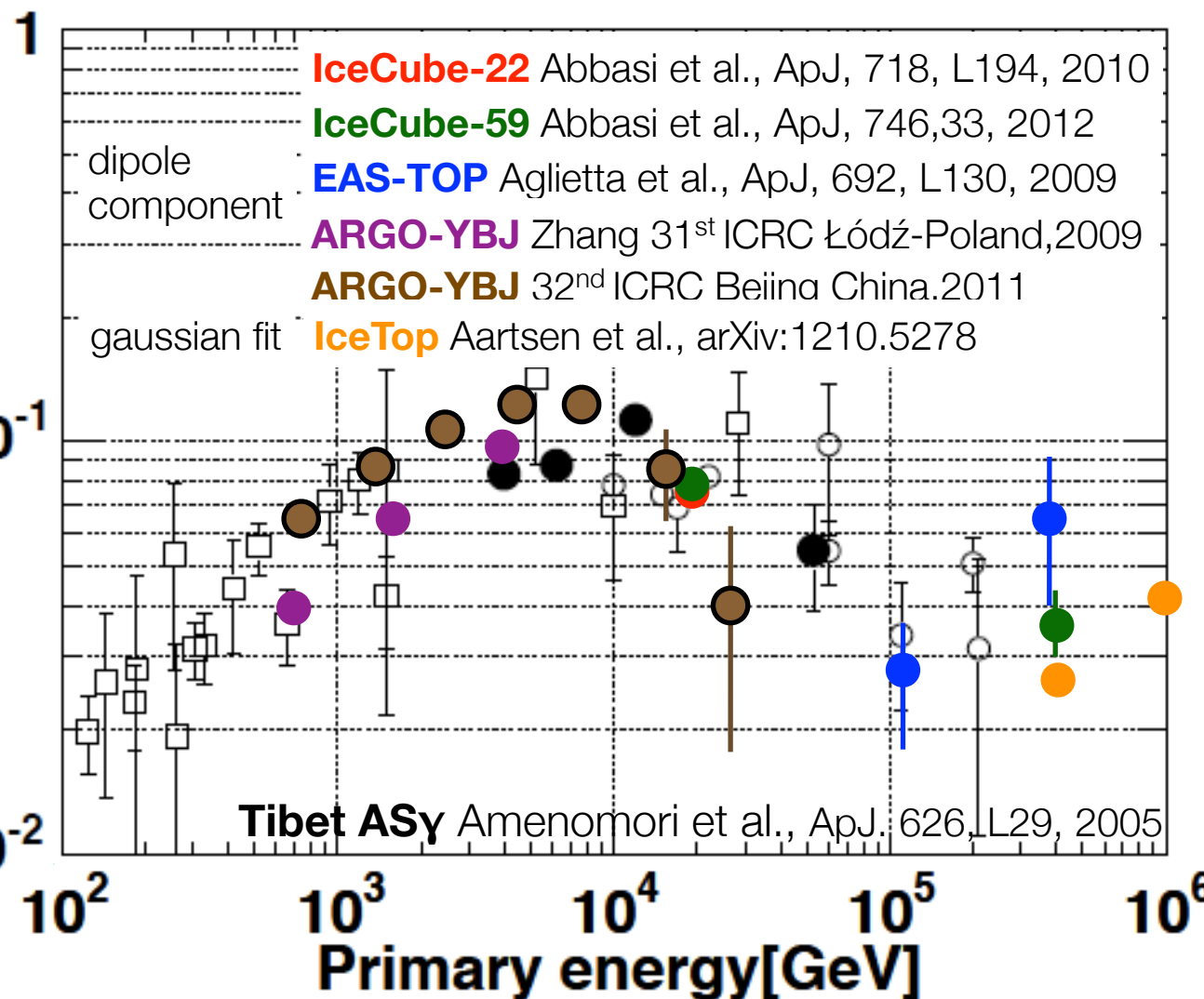


cosmic ray anisotropy



equatorial coordinates

cosmic ray anisotropy large scale energy dependency



$$\delta A = \left| \sum_{SNR} \frac{eD(E)}{c} \cdot \frac{\vec{\nabla} \phi_{CR}}{\phi_{CR}}(E) \right|$$

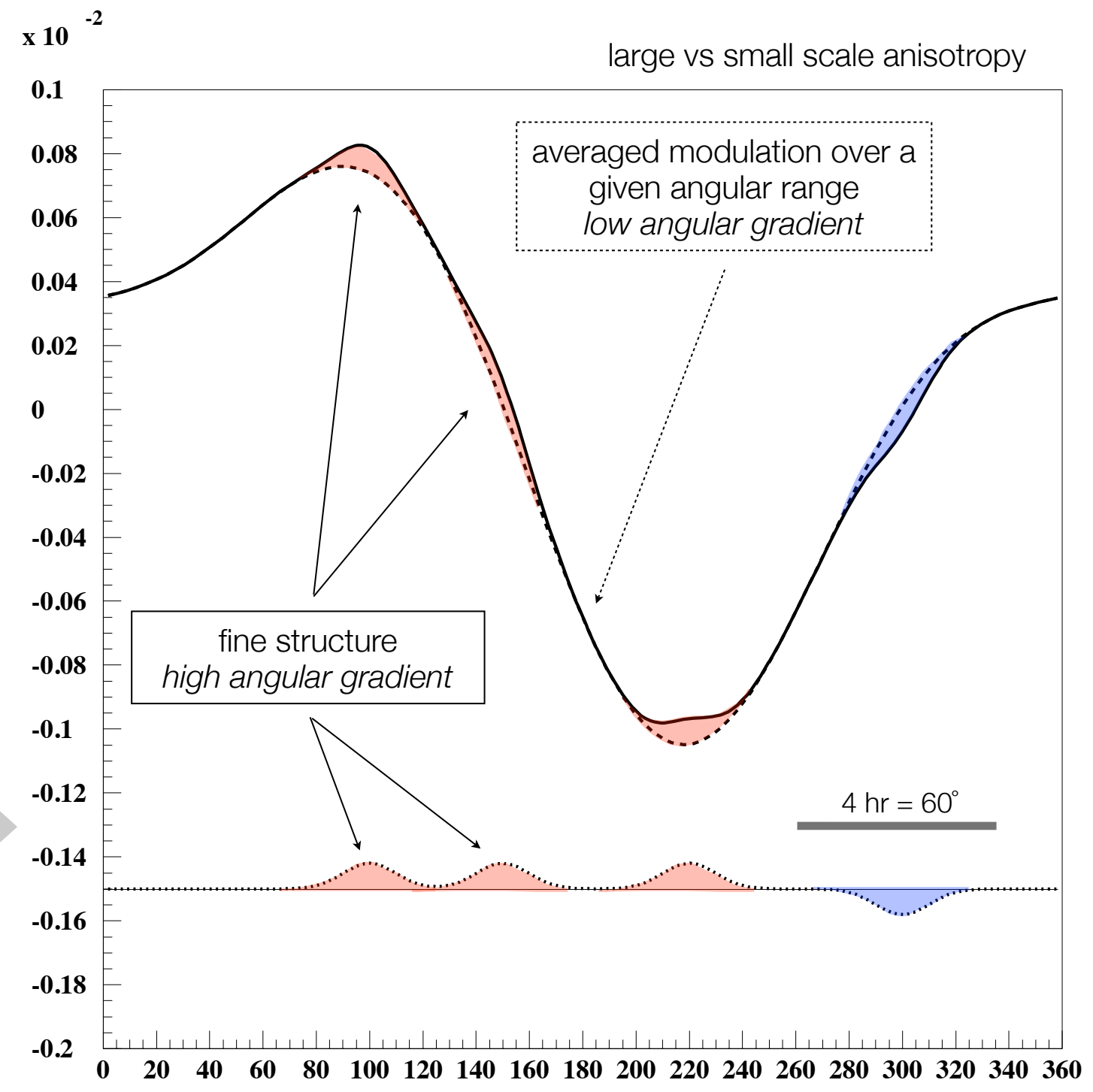
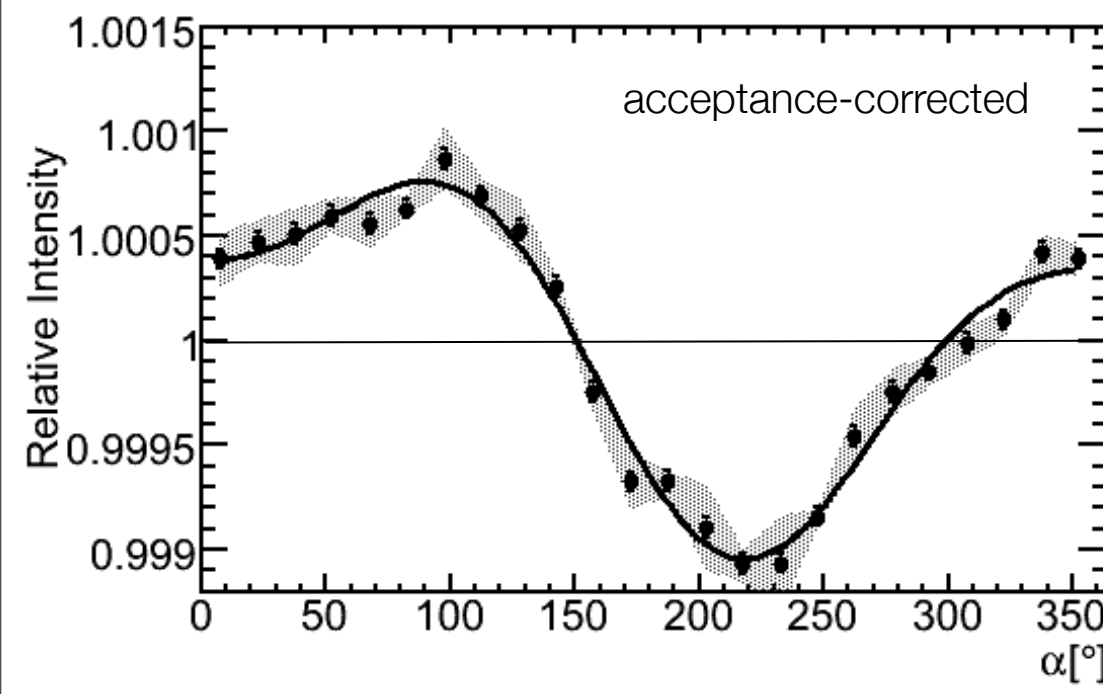
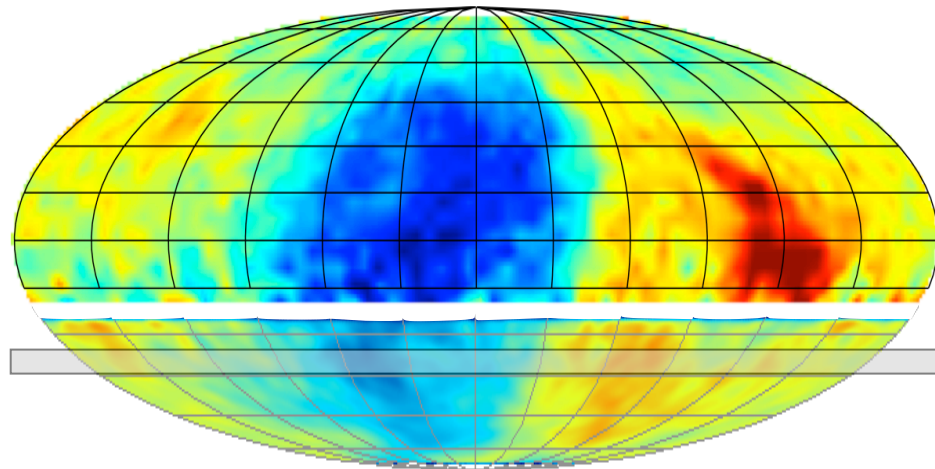
anisotropy amplitude $\sim 10^{-4}$ - 10^{-3}

$$D(E) \approx (3 - 5) \times 10^{28} \cdot E^{0.3 - 0.6} \quad [cm^2 s^{-1}] \quad \text{diffusion coefficient}$$

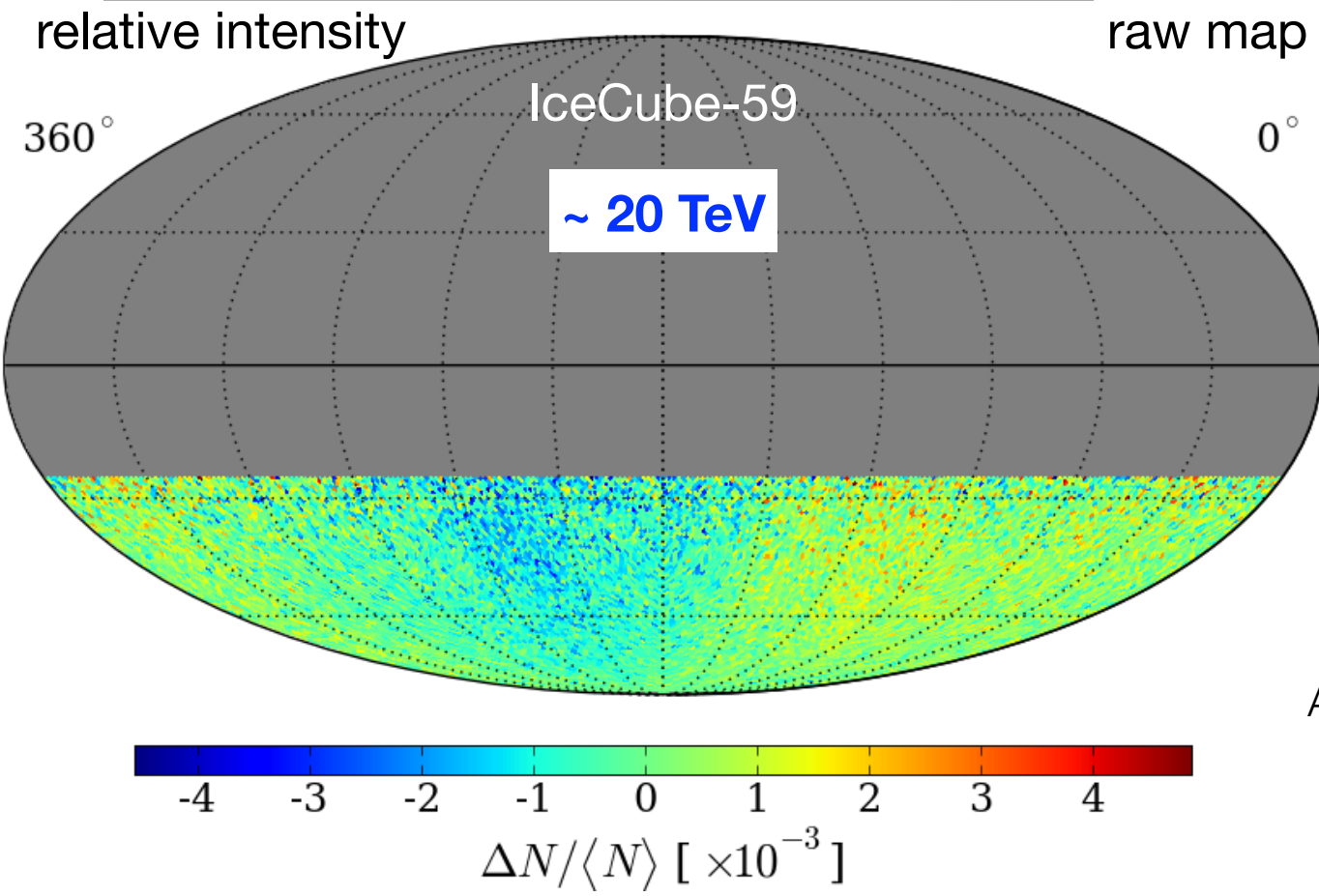
$$\Rightarrow \delta A \propto E^{0.3 - 0.6}$$

anisotropy increases vs energy

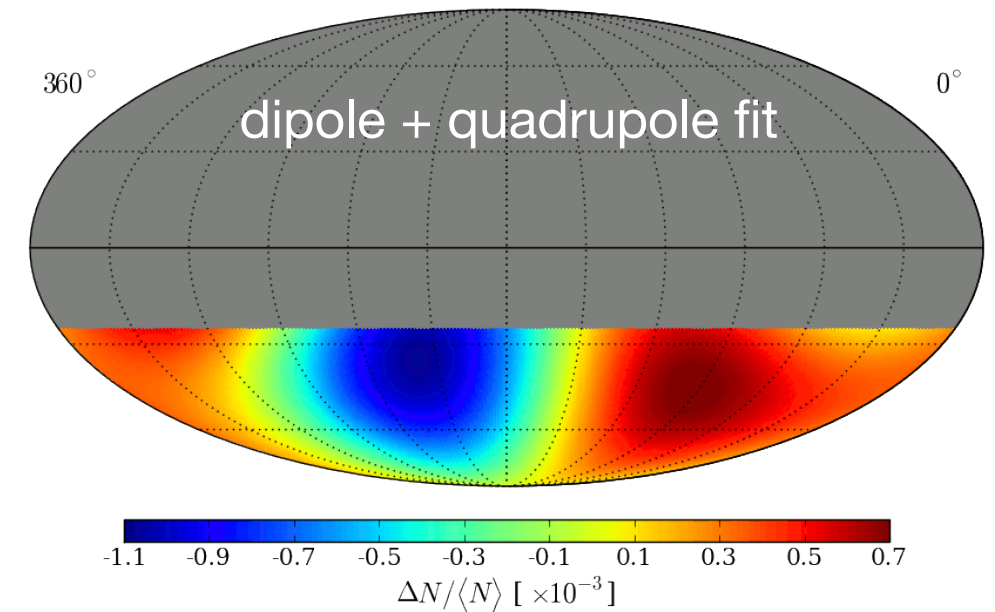
cosmic ray anisotropy angular scale structure



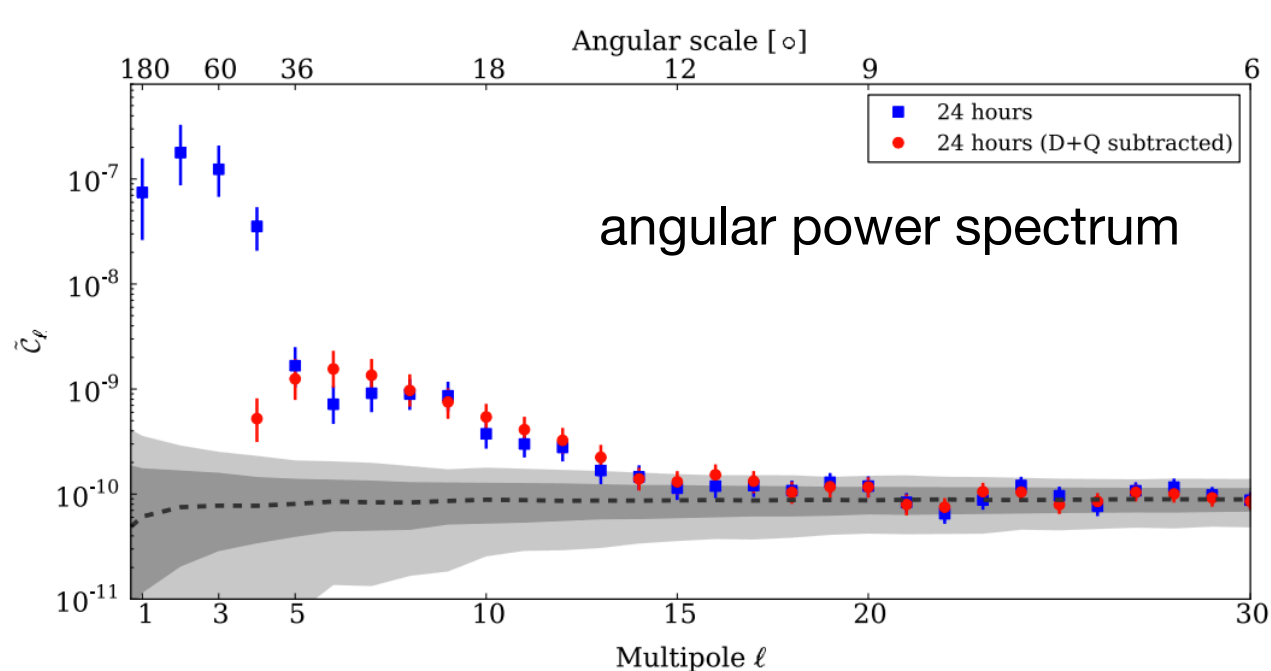
cosmic ray anisotropy small scale IceCube



$\chi^2/\text{ndf} = 14743.4 / 14187$
 $\text{Pr}(\chi^2|\text{ndf}) = 0.05\%$



Abbasi et al., ApJ, 740, 16, 2011



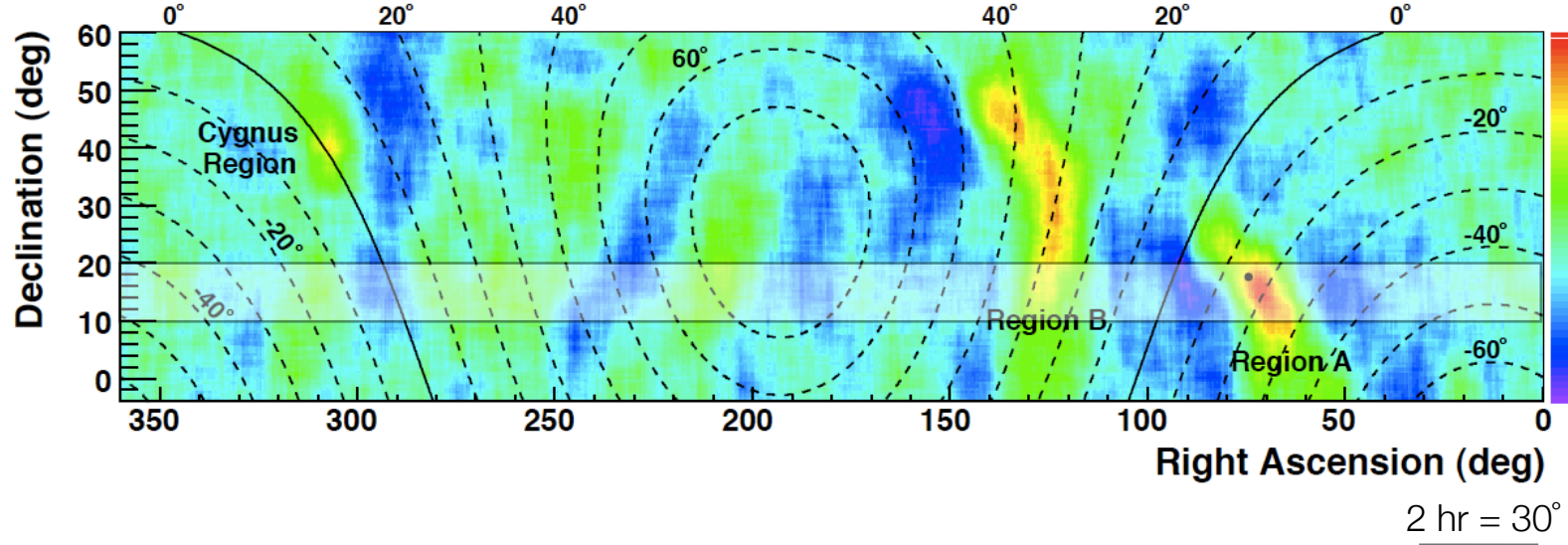
sky map contains correlations at several angular scales
in gray 60% and 95% of simulated isotropic bands

in gray 60% and 95% of simulated isotropic bands

large and small scales separated @ $\sim 20 \text{ TeV}$?

spectral feature associated to anisotropy

Abdo A.A. et al., Phys. Rev. Lett., 101, 221101 (2008)



Milagro

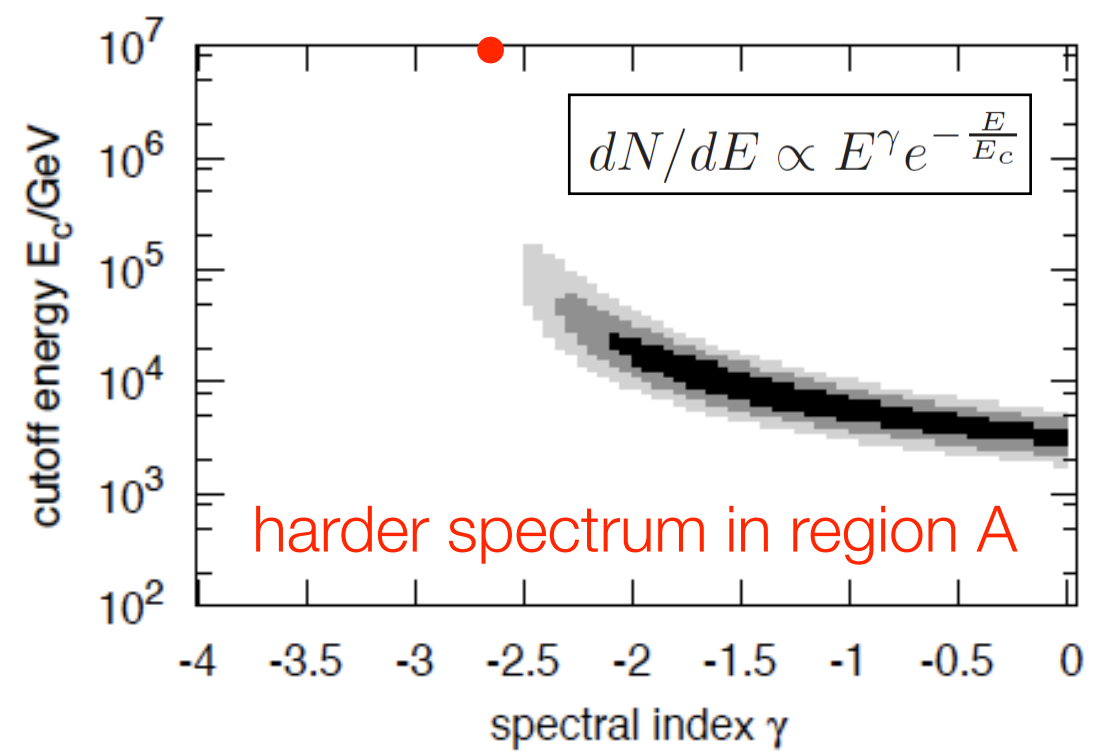
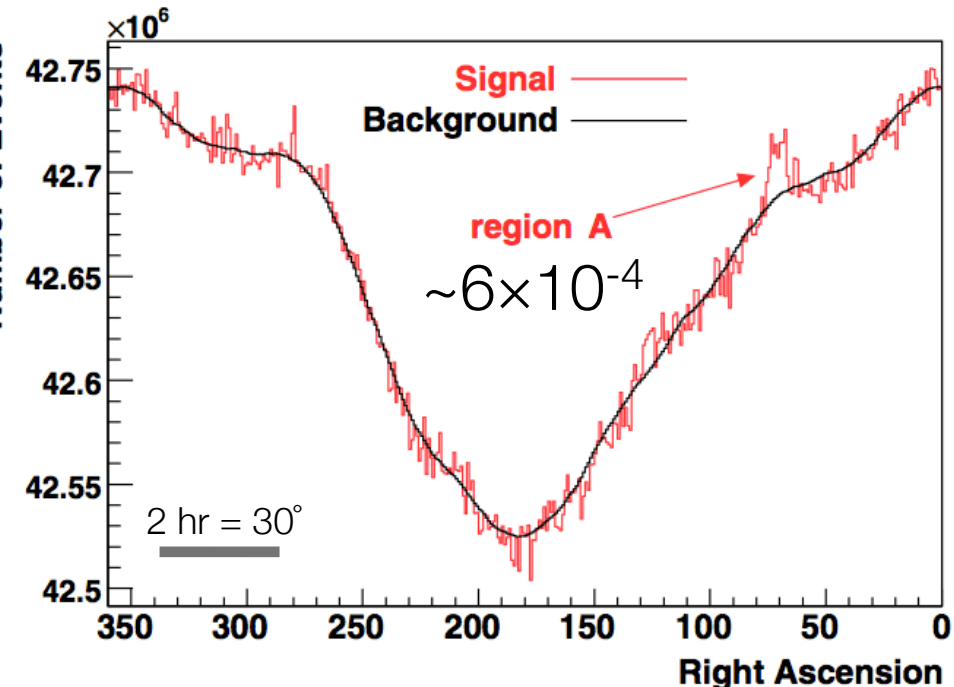
& ARGO-YBJ

Di Sciascio et al., arXiv:1202.3379

harder than average spectrum from region A

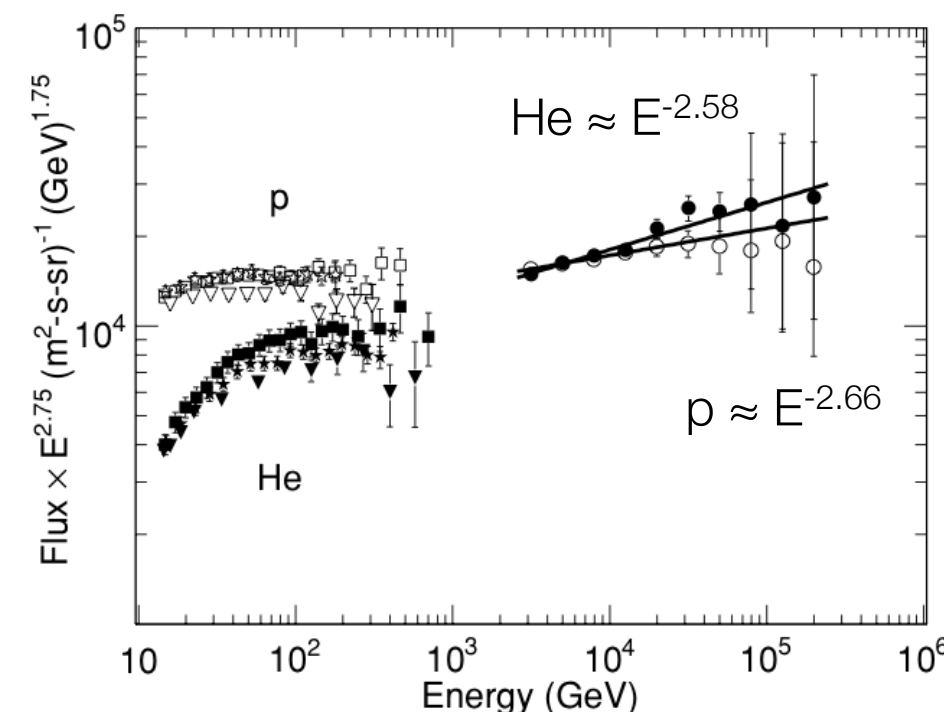
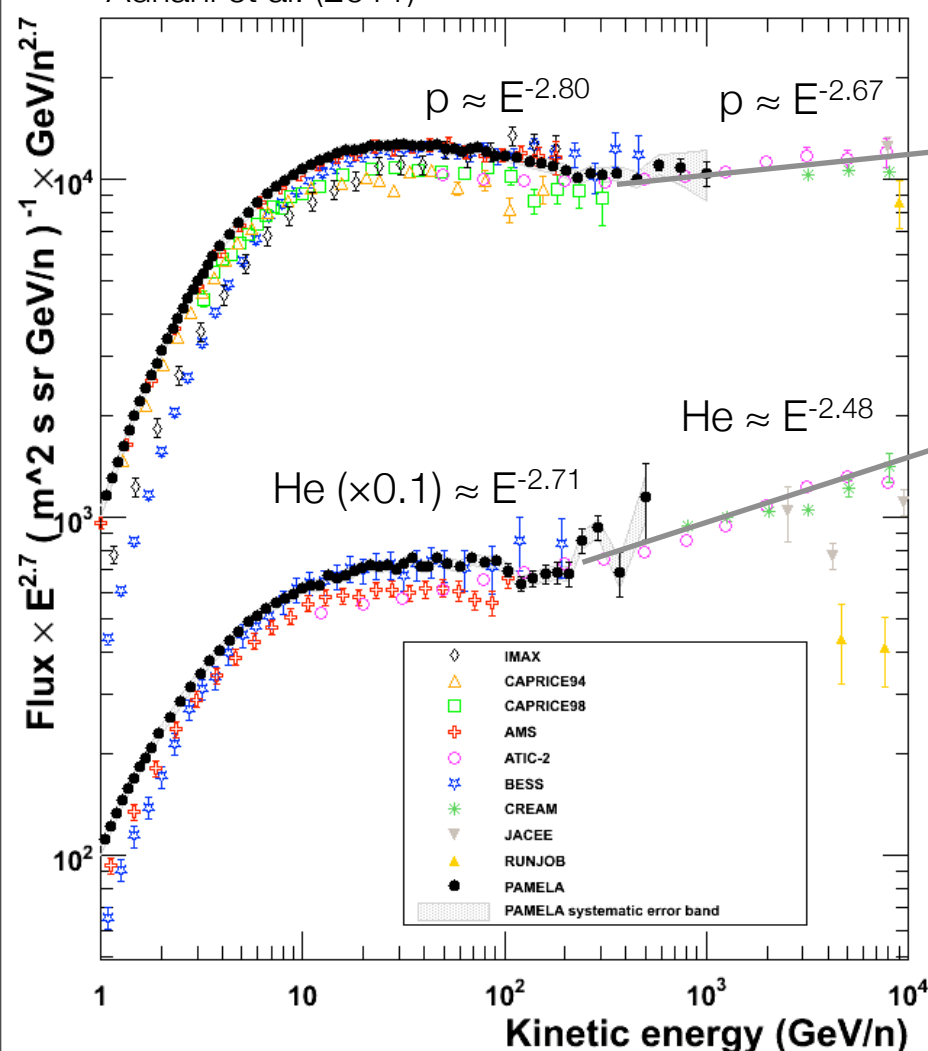
$\gamma < 2.7$ at 4.6σ level
 $E_c = 3 - 25$ TeV

similar to hardening of “diffuse” cosmic rays by Pamela, CREAM, ATIC-2, or something else ?

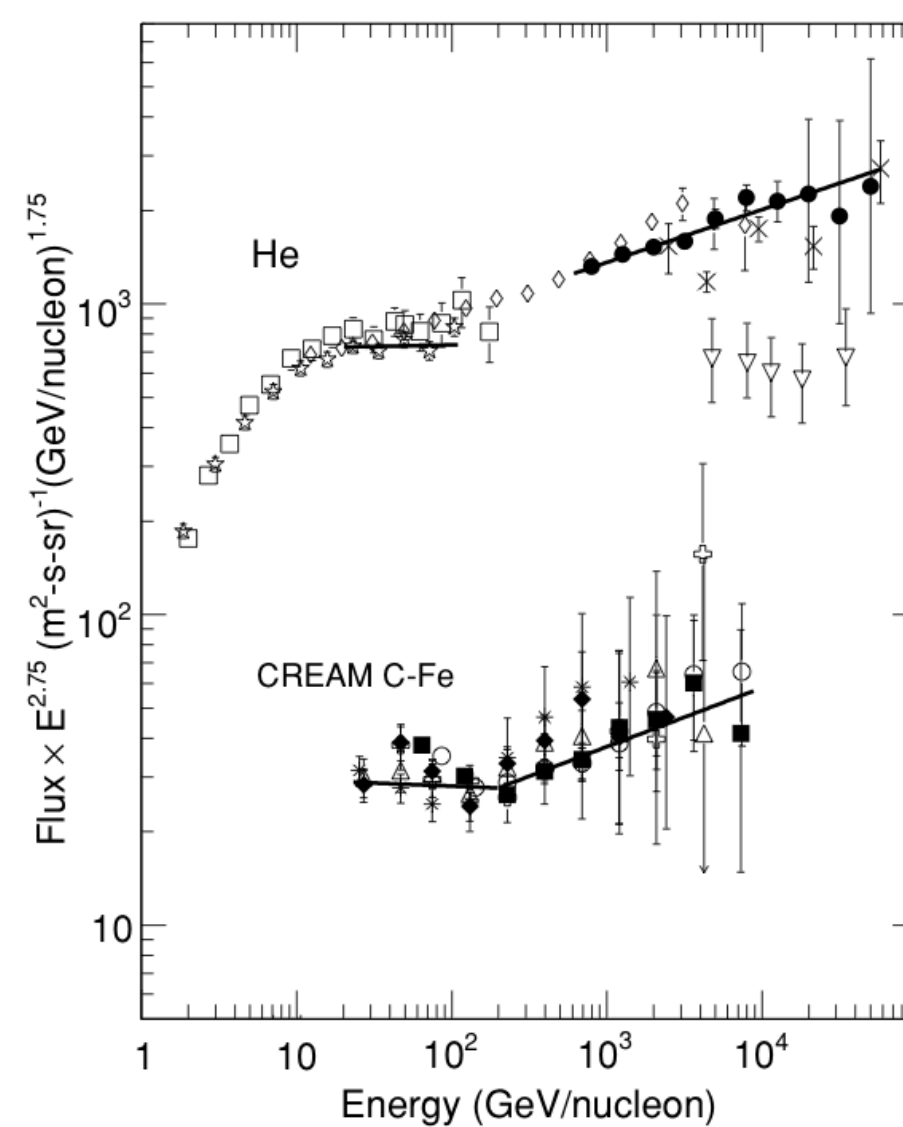


cosmic rays observations all-particle spectrum

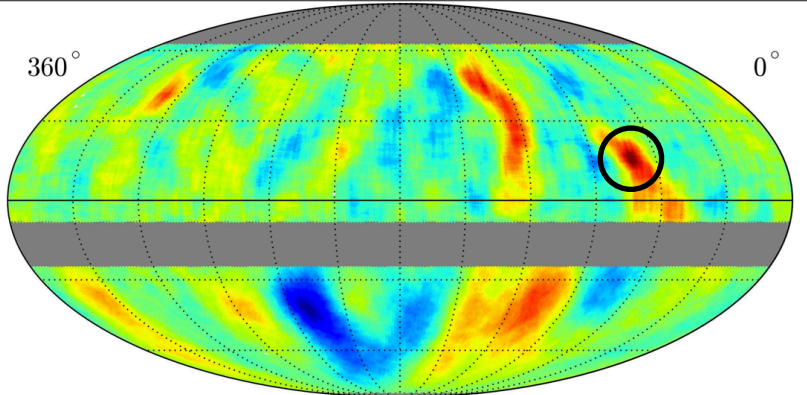
Pamela
Adriani et al. (2011)



CREAM
Ahn et al. (2010)



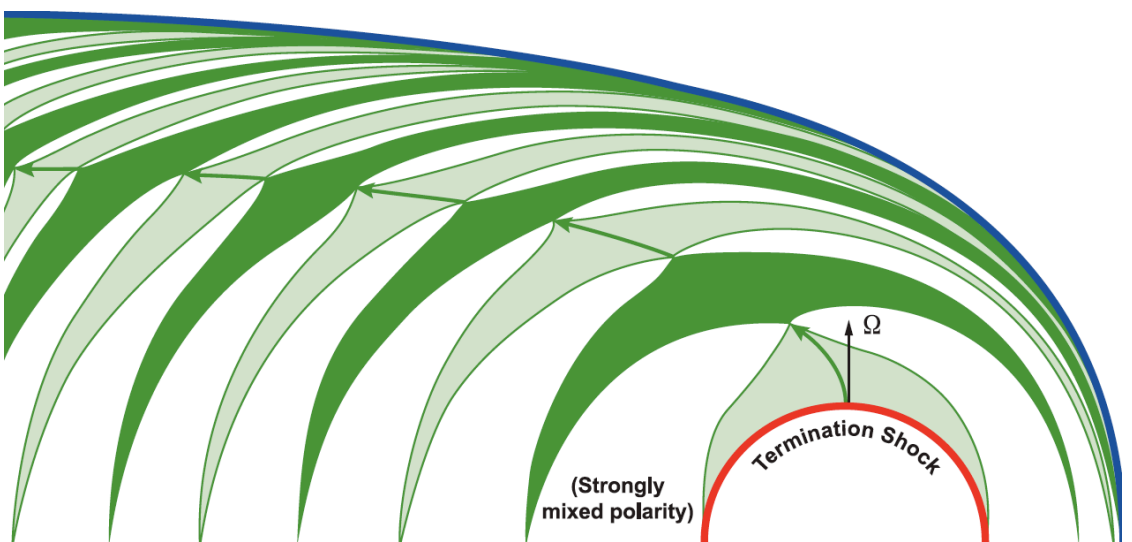
origin of spectral hardening ?



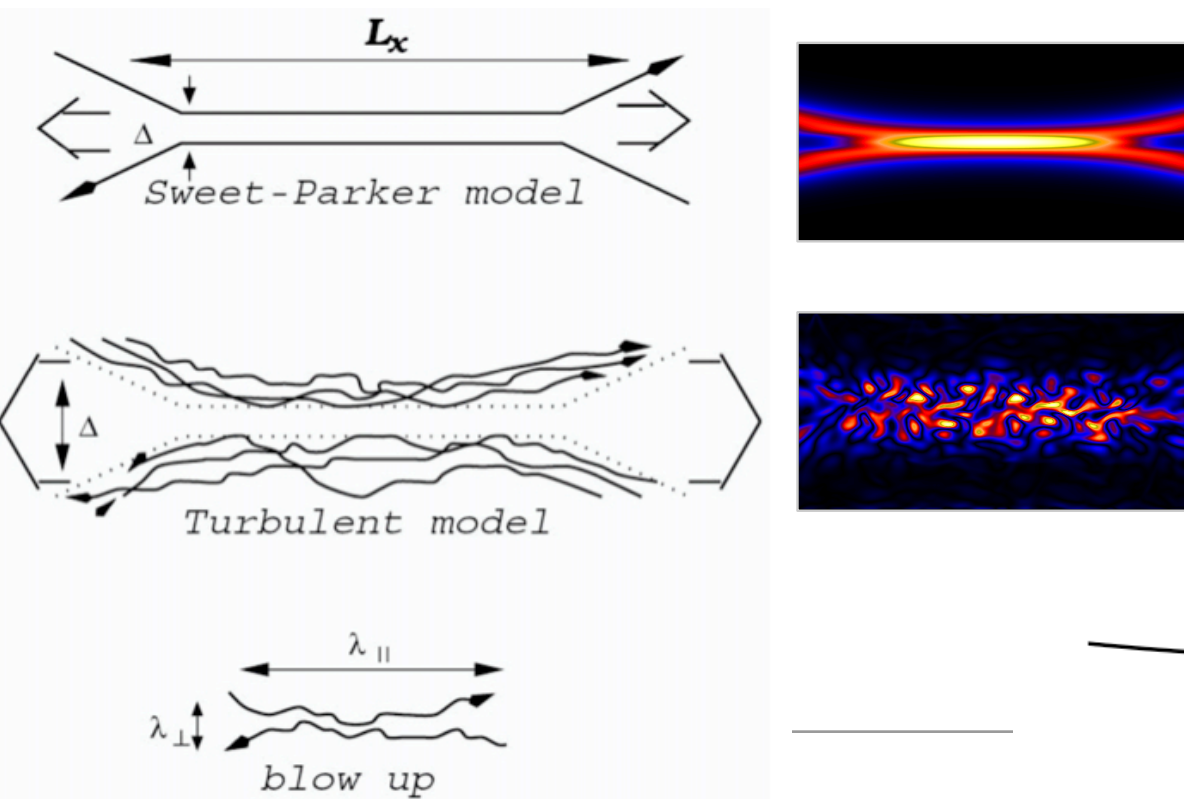
Lazarian & PD, ApJ, 722, 188, 2010

- ▶ magnetic polarity reversals due to the 22-year solar cycles produces large scale sectors
- ▶ converging of turbulent magnetic field lines can trigger reconnection and make it fast
- ▶ magnetic mirror @ single reconnection as site of acceleration (test particle)

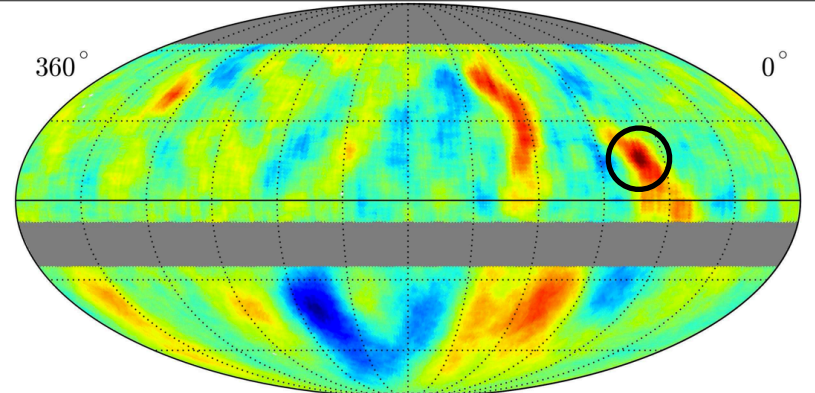
Sweet (1959) & Parker (1957)



Lazarian & Vishniac, ApJ, 517, 700 (1999)



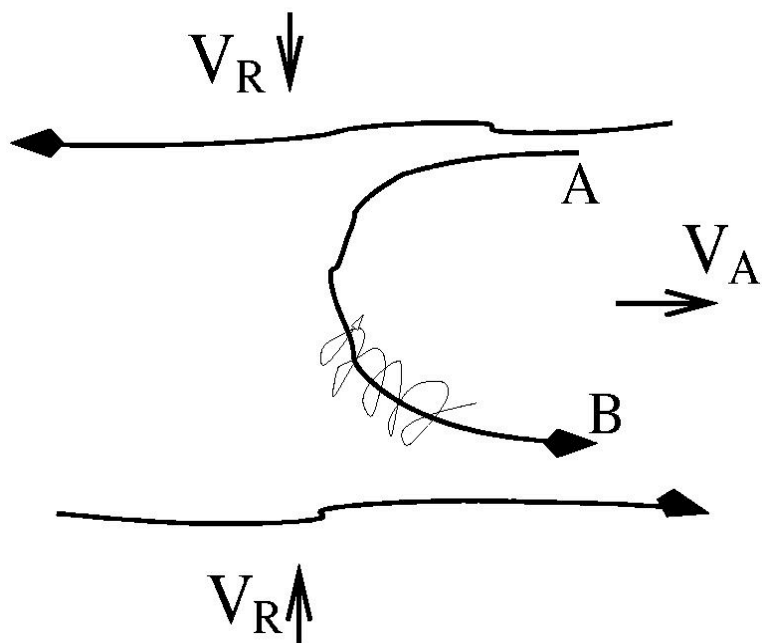
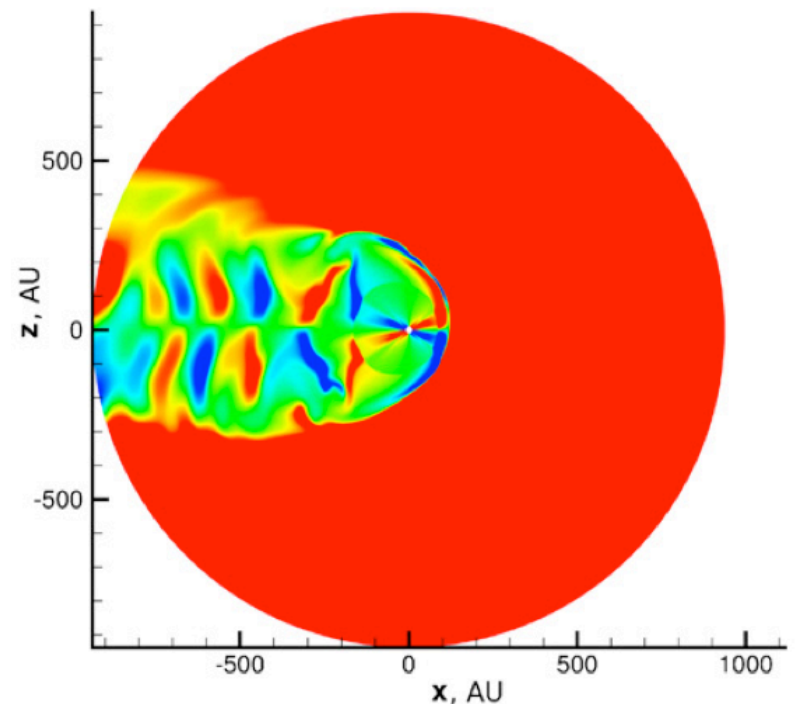
stochastic magnetic reconnection

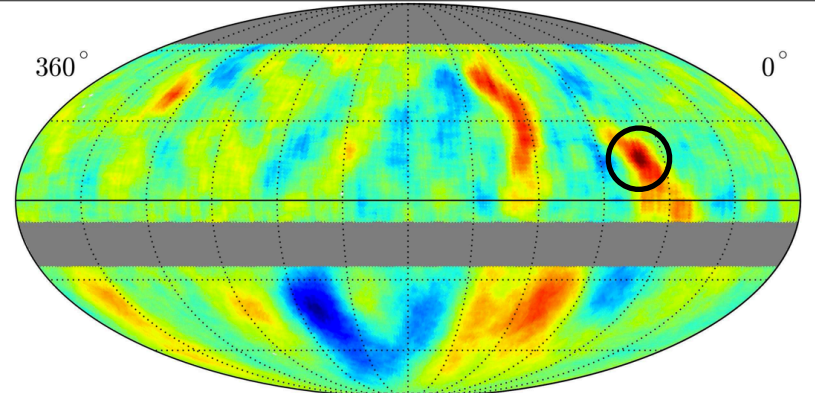


Lazarian & PD, ApJ, 722, 188, 2010

- ▶ magnetic polarity reversals due to the 22-year solar cycles produces large scale sectors
- ▶ converging of turbulent magnetic field lines can trigger reconnection and make it fast
- ▶ magnetic mirror @ single reconnection as site of acceleration (test particle)
- ▶ 1st order Fermi acceleration

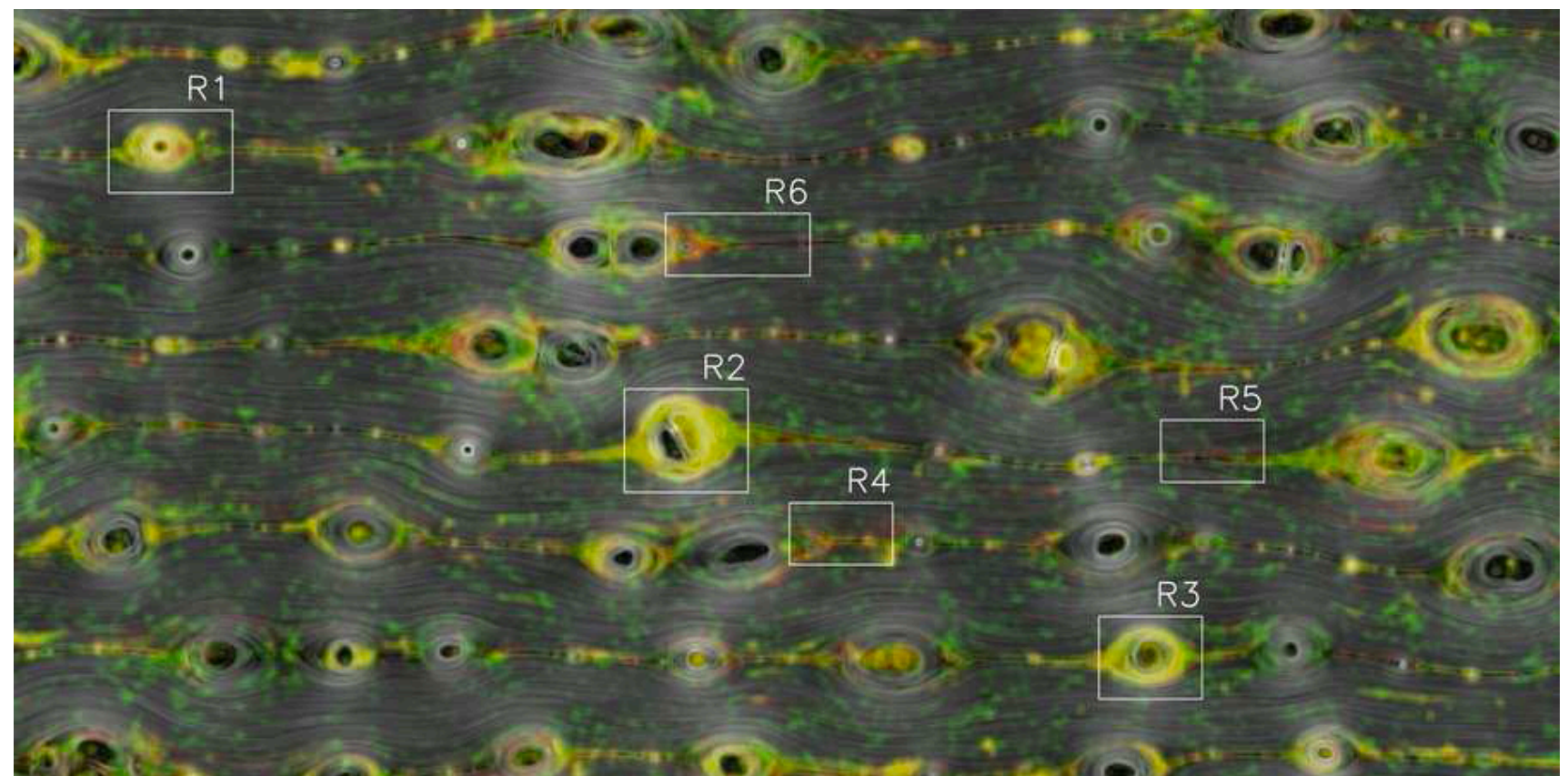
$$N(E) dE \sim E^{-5/2} dE$$



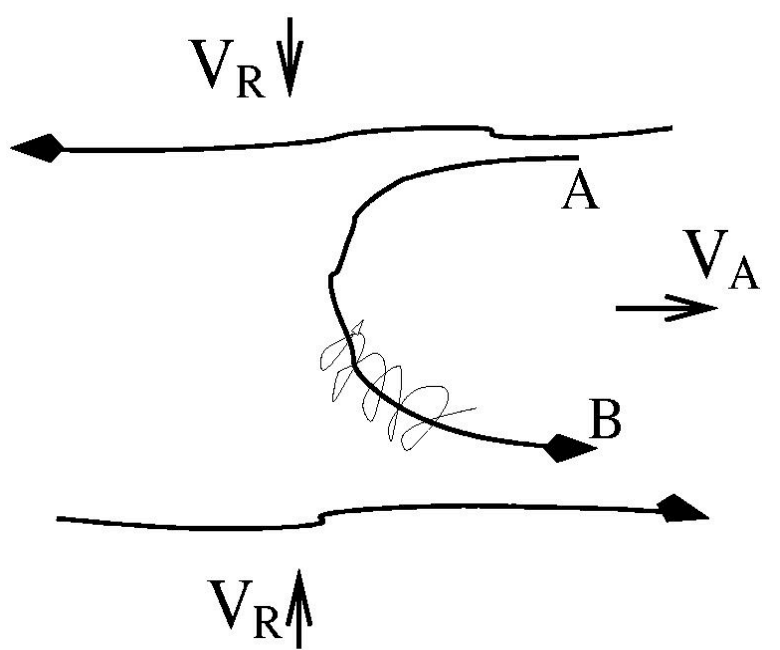


stochastic magnetic reconnection

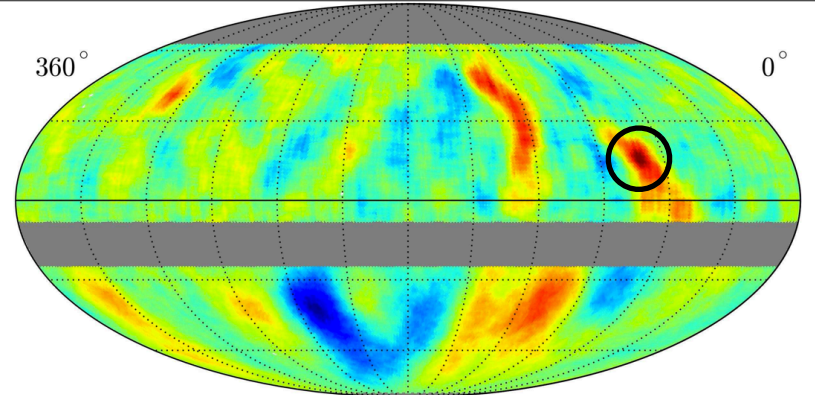
Kowal et al., ApJ 735, 102 (2011)



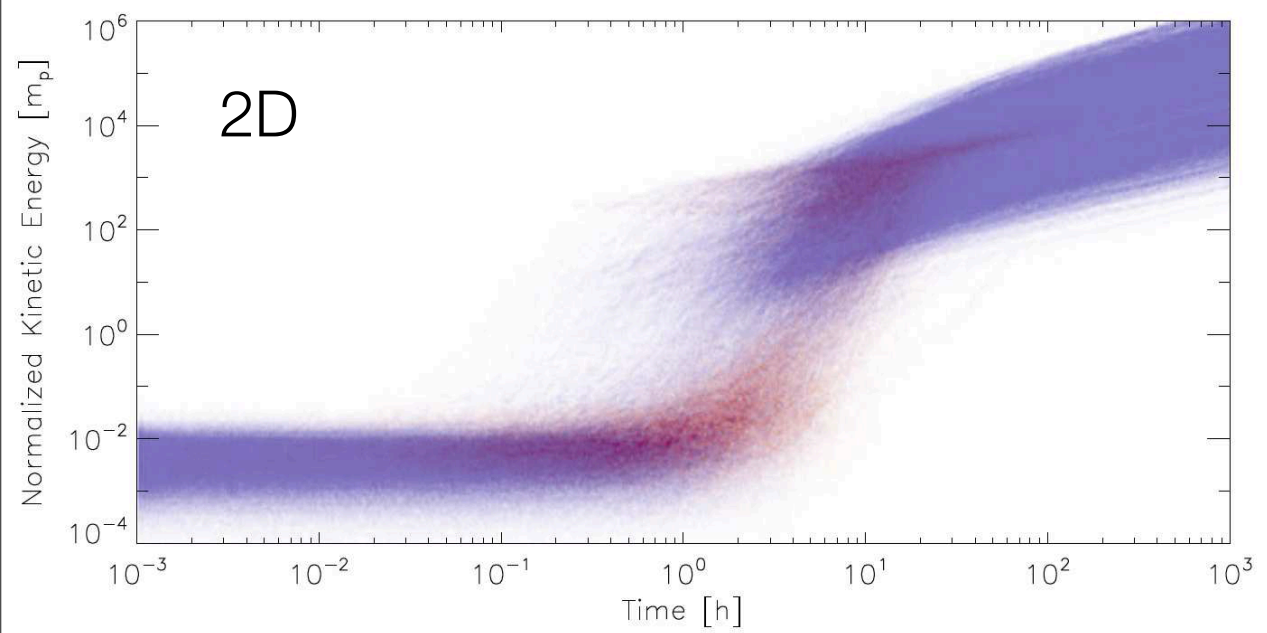
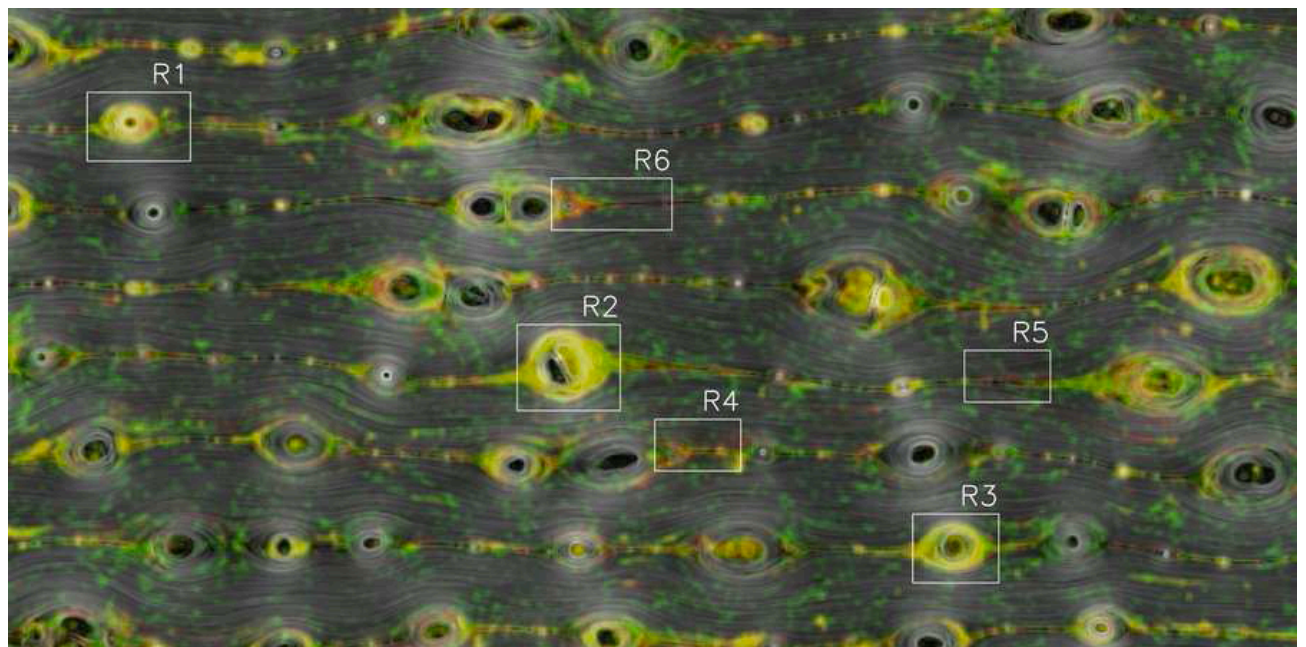
$$N(E) dE \sim E^{-5/2} dE$$



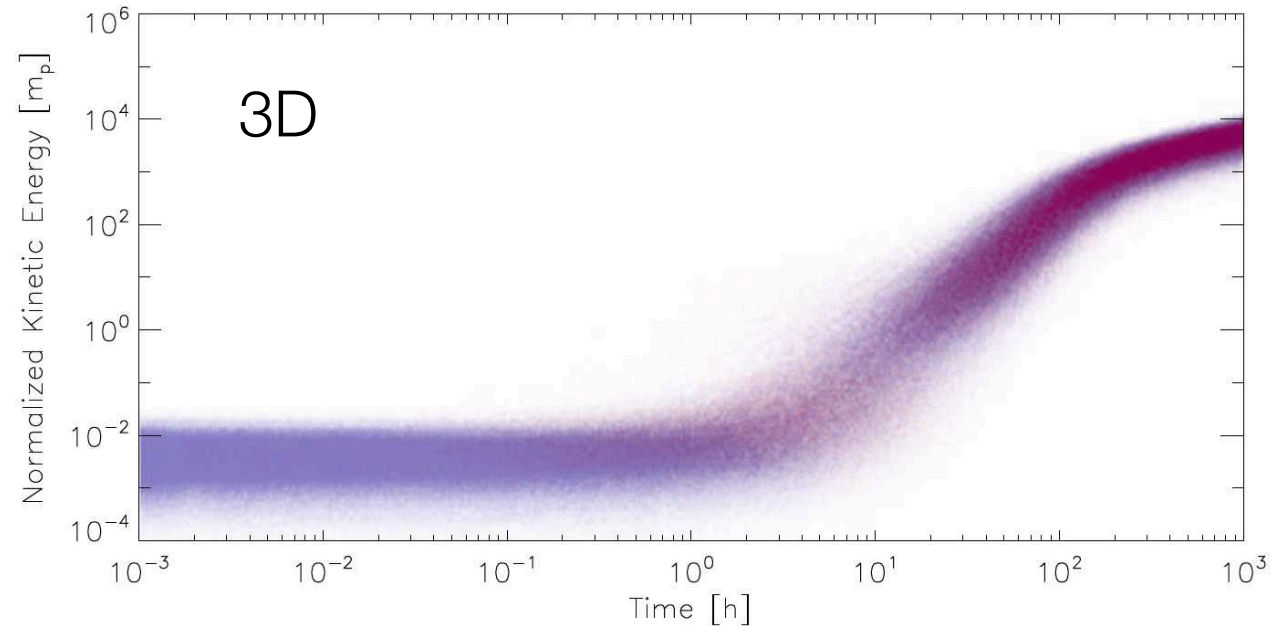
stochastic magnetic reconnection



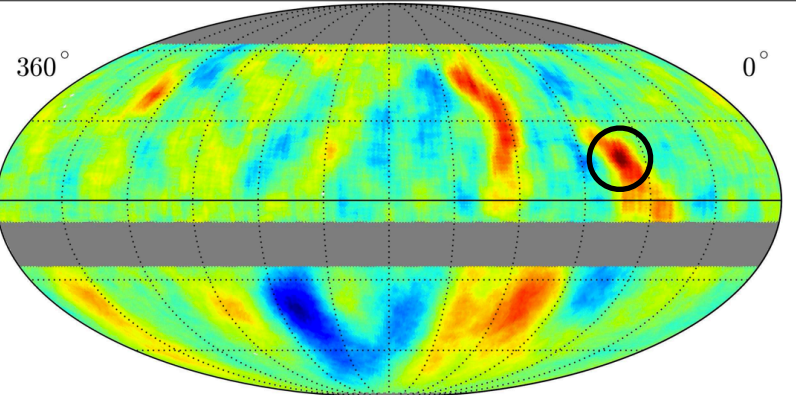
Kowal et al., ApJ 735, 102 (2011)



$$\mathbf{V}_\perp > \mathbf{V}_\parallel$$



$$\mathbf{V}_\parallel > \mathbf{V}_\perp$$

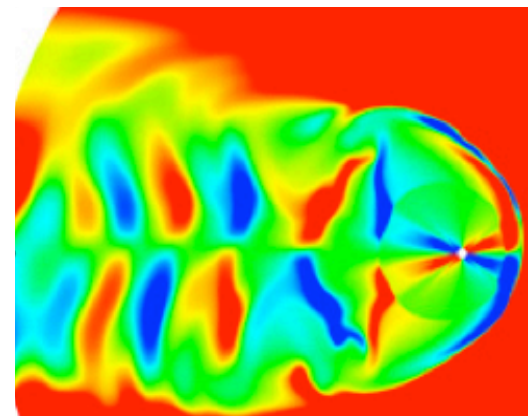


stochastic magnetic reconnection

- ▶ 2nd order Fermi acceleration is dominant in purely turbulent plasmas with no converging magnetic flow

Kowal et al., PRL 2012

- ▶ if converging flow occurs 1st order Fermi acceleration is the most important
- ▶ acceleration by reconnection is efficient if scattering does not isotropize particles. Scattering expected to be minimal along the tail line of sight

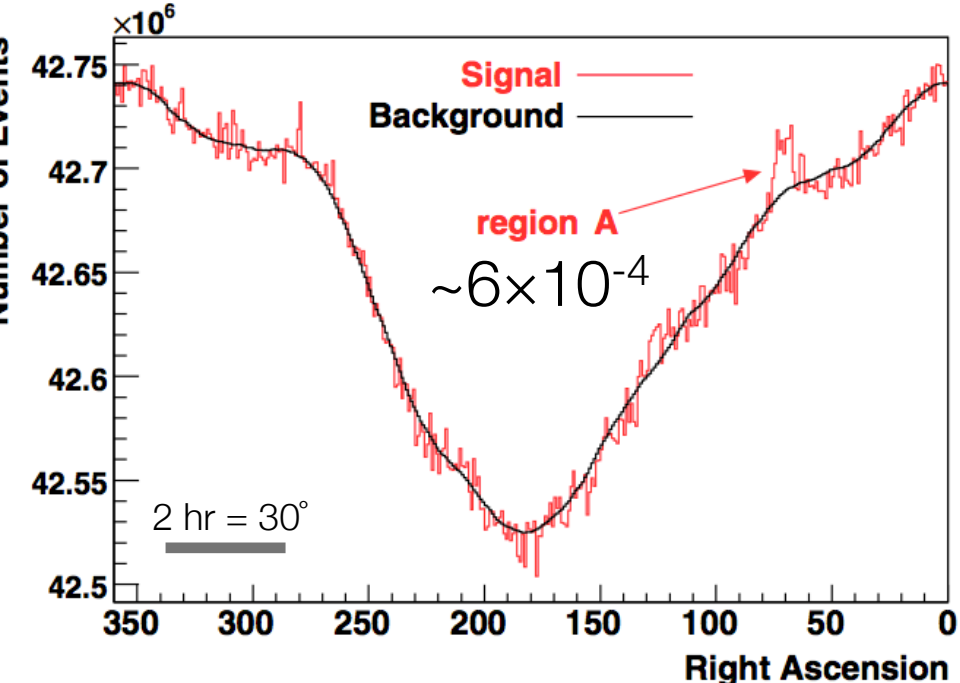
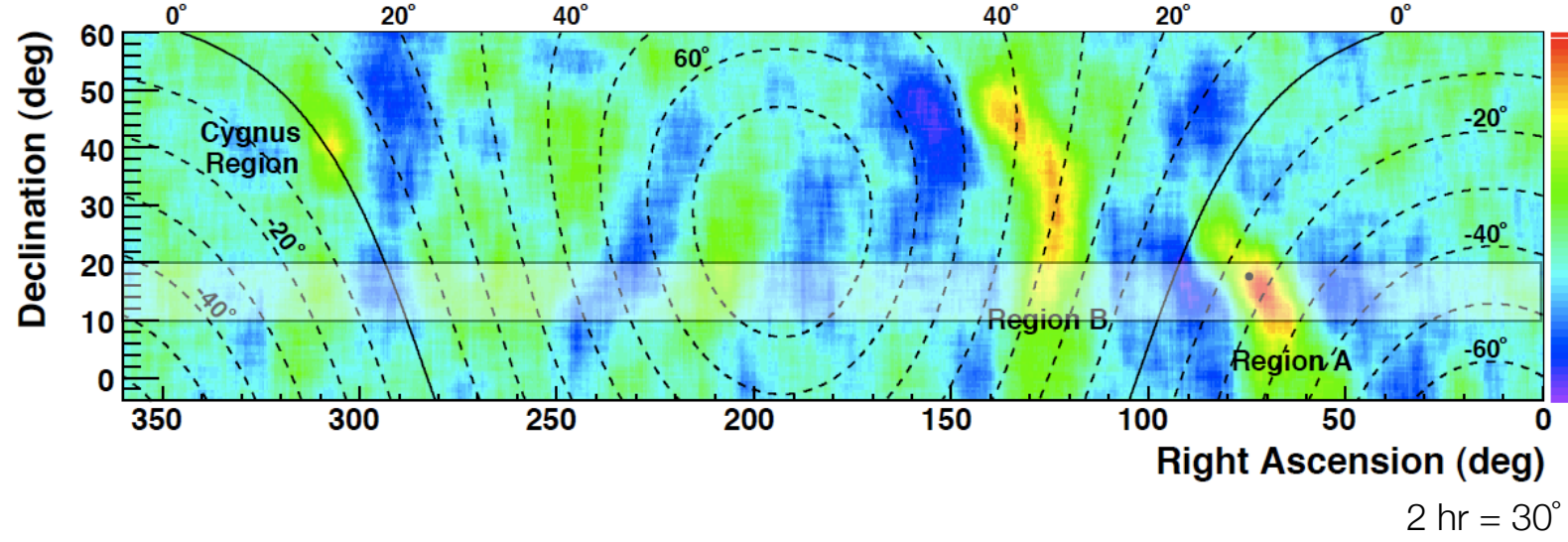


$$E_{max} \approx 0.5 \left(\frac{B}{1 \mu G} \right) \left(\frac{L_{zone}}{100 AU} \right) TeV \approx 0.5 - 6 TeV$$

- ▶ cosmic rays re-accelerated as long as trapped in large scale reconnection regions

spectral feature associated to anisotropy

Abdo A.A. et al., Phys. Rev. Lett., 101, 221101 (2008)



Milagro

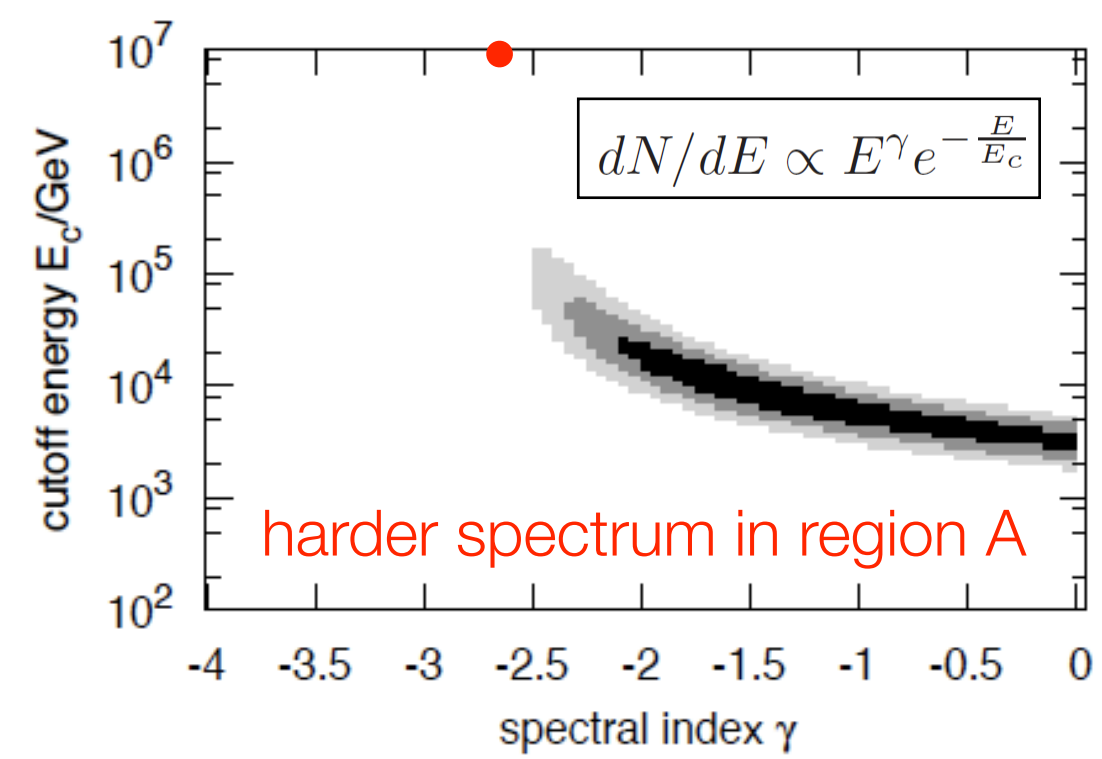
$\gamma < 2.7$ at 4.6σ level
 $E_c = 3 - 25$ TeV

$E_{\text{flux}}(10\text{GeV}-10\text{TeV}) \sim 10^{-9} - 10^{-8}$ erg cm⁻² s⁻¹ ($\gamma = 2.7 - 2.0$)

$\langle P_{\text{re-acc}} \rangle \sim 10^{20} - 10^{22}$ erg s⁻¹

$\langle P_{\text{solar wind}} \rangle \sim 10^{27}$ erg s⁻¹

(Parker, 1962)



PD, Lazarian, NPG, **19**, 1, 2012

cosmic ray anisotropy astrophysical origin ?

- stochastic effect of recent nearby CR sources
 - ▶ influences spectrum and global arrival direction
 - ▶ diffusive scenarios to explain observed features
- propagation effects in turbulent ISMF
- convection from persistent magnetized flow field from old SNRs
- breakdown of diffusion regime via scattering with ISMF turbulence

Dorman+ 1985
Ptuskin+ 2006
Erlykin & Wolfendale 1997, 2001, 2006
Sveshnikova+ 2013
Blasi & Amato 2011, 2012
Pohl & Eichler 2012

Salvati & Sacco 2008
Drury & Aharonian 2008
Salvati 2010

Battaner+ 2009
Malkov+ 2010

Biermann+ 2012

Giacinti & Sigl 2011

- ▶ diffusion cannot explain the observed **non-dipolar** topology & **small angular scales**
- ▶ limitations on single power-law assumption and spacial dependency of diffusion coeff.

scattering on heliospheric boundary toy model

PD & Lazarian, ApJ, **762**, 44, 2013

$$N_b = n_{\text{CR}} P_s R_E^2 \int_{R_H}^{R_H+dR_H} dr \int_0^{2\pi r} dl \int_0^\infty \frac{dz}{z^2 + r^2}$$

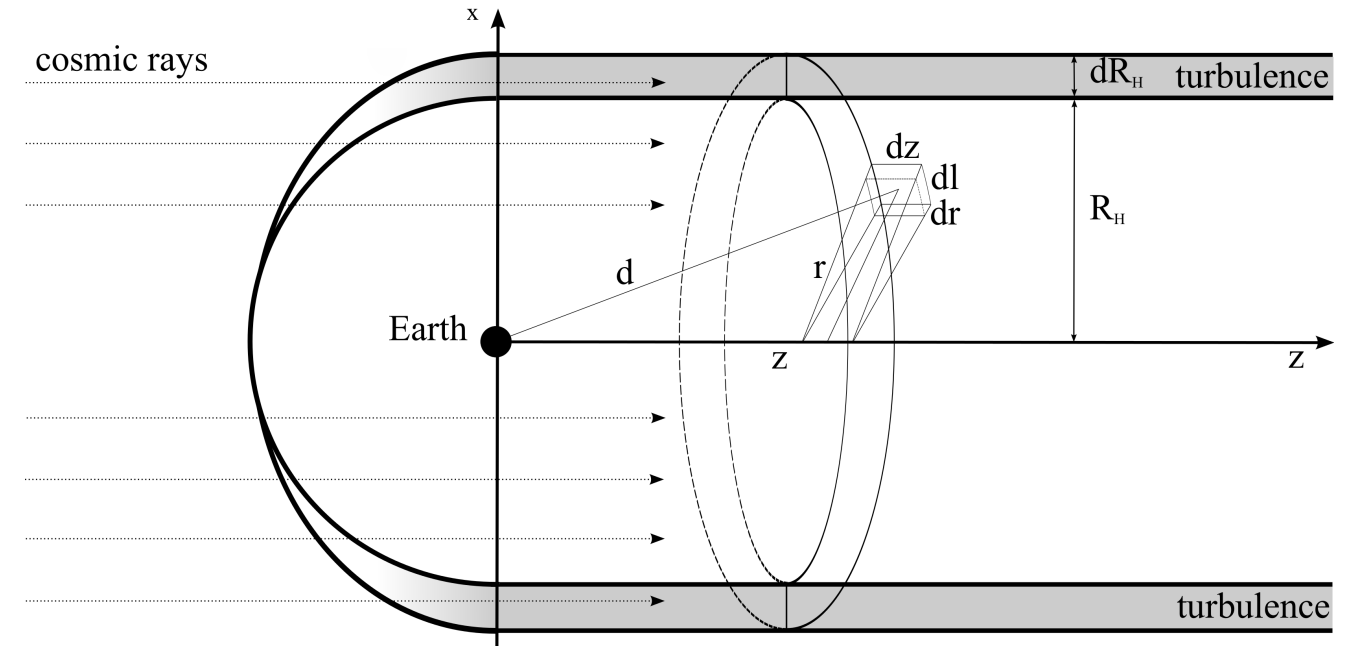
$$= n_{\text{CR}} P_s \pi^2 R_E^2 dR_H,$$

$$N_d = n_{\text{CR}} 4\pi R_E^2 c \tau.$$

$$\delta = \frac{N_b - N_d}{N_b + N_d} = \frac{N_b/N_d - 1}{N_b/N_d + 1},$$

$$\frac{N_b}{N_d} = \frac{3\pi}{4} P_s \frac{dR_H}{c \tau}.$$

$$\delta \gtrsim 0, \quad P_s \gtrsim 100/dR_H$$

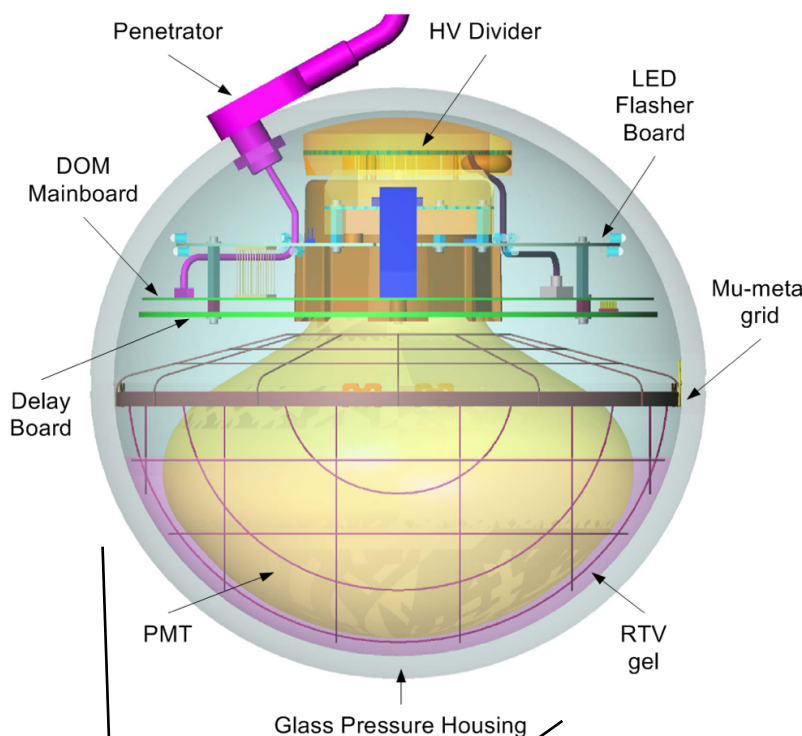


IceCube Observatory

air shower detection @ 2835 m altitude (680 g/cm²)

muon detection @ 1450-2450 m depth

Digital Optical Module - DOM
with 10" PMT &
local DAQ electronics



IceCube Lab

50 m

450 m

2450 m

2820 m

Bedrock

IceTop
81 Stations, each with
2 IceTop Cherenkov detector tanks
2 optical sensors per tank
324 optical sensors

IceCube Array
86 strings including 8 DeepCore strings
60 optical sensors on each string
5160 optical sensors

December, 2010: Project completed, 86 strings

DeepCore
8 strings-spacing optimized for lower energies
480 optical sensors

Eiffel Tower
324 m

detection principle

